PB-230 418

FIELD INVESTIGATION OF MIXING AND DISPERSION IN A DEEP RESERVOIR

Joe R. Wilson, et al

Texas University
Austin, Texas

June 1967

DISTRIBUTED BY:

NTIS

National Technical Information Service
U. S. DEPARTMENT OF COMMERCE
5285 Port Royal Road, Springfield Va. 22151

PB 230 418

FIELD INVESTIGATION OF MIXING AND DISPERSION IN A DEEP RESERVOIR

by

Joe R. Wilson
and
Frank D. Masch

submitted under
Grant 5 RO1 WP00705
Federal Water Pollution Administration

HYDRAULIC ENGINEERING LABORATORY
Department of Civil Engineering
THE UNIVERSITY OF TEXAS
Austin, Texas 78712

Tech. Rep. Hyd 10-6701

June, 1967

PREFACE

This report is submitted under Grant 5 RO1 WP00705-02 with the Federal Water Pollution Control Administration. The work was originally begun under Grant WP00705-01A1 with the United States Public Health Service. These grants provide for an investigation of the mixing and dispersion processes in reservoirs.

The work reported herein involves a field investigation of the dispersion of a conservative tracer in a fresh water reservoir where the predominant currents were generated by wind. The purposes of the investigation were to explore various measuring techniques and to examine velocity distributions, rate of dilution and dispersion coefficients and their relation to surface currents and various wind-wave conditions.

The authors are grateful to several individuals for their help in the research reported herein and in the preparation of the final report. Special thanks go to Drs. E. F. Gloyna, W. L. Moore, Joe O. Ledbetter and R. T. Gregory with whom several thought-provoking sessions were held. Field and laboratory assistance was provided by Mssrs. Tom Gebhard and Ed Bruce. Special thanks also go to the Bureau of Engineering Research at The University of Texas and Mr. Dale Bergman for the drafting and Miss Toni Daleo for typing the manuscript.

The financial support from the United States Public Health Service and the Federal Water Pollution Control Administration which has made this study possible is also gratefully acknowledged.

ABSTRACT

A field investigation of the dispersion of a conservative tracer was made in a fresh water reservoir in which the predominant currents are generated by the wind. The purpose of the investigation was to examine the current velocity distribution with depth, the rate of dilution and the dispersion coefficients for correlation with such parameters as the surface current velocity and the wave conditions.

Tests were conducted at three sites of very different geometric characteristics in Lake Travis near Austin, Texas. Rhodamine B, a fluorescent organic dye, was used as the tracer. Detection was accomplished with a Turner model 111 fluorometer. The study was limited to time scales of less than six hours and to dye releases at the surface only.

The results show that the vertical and lateral diffusivities increase with the energy in the wave spectrum, but that the longitudinal diffusivity decreases. The dominant mechanism for dispersion is the shear flow mixing resulting from the spatial variation in the direction and/or the magnitude of the currents. Velocity studies showed that near the surface the velocity diminishes rapidly with depth. In this zone, the shear flow mixing accounts for most of the dispersion.

The peak concentration in a dispersing cloud was found to decrease as the minus 2.5 power of time. This rate is independent of

Preceding page blank

the ambient conditions and of the geometric characteristics of the site. The peak concentration, C, at time, t, in a dispersing cloud may be predicted by the empirical formula:

$$C = C_o \alpha t^{2.5} \qquad (4\text{-}11)$$

where C_o is the initial concentration of the tracer introduced at zero time, and α is a dilution coefficient to account for turbulence.

Preceding page blank

TABLE OF CONTENTS

Preface iii

Abstract iv

List of Figures xi

List of Symbols viii

CHAPTER 1. Introduction 1

1-1 General 1

1-2 Objectives and Scope 3

CHAPTER 2. Background 6

2-1 Theoretical Background 6

2-2 Previous Experimental Efforts 24

CHAPTER 3. Equipment and Techniques 29

3-1 Tracer 29

3-2 Fluorometer 31

3-3 Arrangement of Equipment for Continuous Sampling 35

3-4 Discrete Vertical Sampling Device 39

3-5 Wave Gage 41

3-6 Drogues 43

3-7 Equipment Calibration 44

3-8 Experimental Methods 48

3-9 Test Sites..... 50

CHAPTER 4. Experimental Observations and Results..... 53

4-1 General..... 53

4-2 Difficulties Encountered..... 54

4-3 Continuous Flow Source versus Instantaneous Release..... 56

4-4 Velocity Distribution..... 59

4-5 Dilution Rate..... 63

4-6 Vertical Dispersion..... 76

4-7 Lateral Dispersion..... 85

4-8 Longitudinal Dispersion..... 92

CHAPTER 5. Conclusions..... 100

CHAPTER 6. Recommendations for Future Research..... 104

Bibliography..... 138

APPENDIX A: Velocity Distribution Test Data..... 105

APPENDIX B: Horizontal Dispersion Test Data..... 107

APPENDIX C: Vertical Dispersion Test Data..... 116

APPENDIX D: Dilution Rate Test Data..... 128

LIST OF SYMBOLS

A	Area
c	Concentration or intensity of fluid property
c_{max}	Maximum or peak concentration
c_o	Initial concentration
D	Coefficient of diffusion or diffusivity
D_x, D_y, D_z	Dispersion coefficients along the x, y, and z axes, respectively
E	Energy dissipation per unit mass
F	Fluorometer reading
F_s	Fluorometer reading at standard temperature
$F(l)$	Richardson's variable diffusion coefficient
$f(r/r_o)$	Universal velocity distribution coefficient
g_x	Csanady's gustiness coefficient
H	Wave Height
h	Depth
K_c	Factor for surface conditions
k, k_1, k_2	Coefficients
l	Mixing length or neighbor separation
M	Diffusant transfer rate
N	Power term in Ippen's Eulerian correlation coefficient
n	Exponent
p	Diffusion velocity parameter

q	Average number of diffusing particles (neighbors) per unit length along the axis of diffusion
R	Correlation coefficient
$R(\xi)$	Lagrangian correlation coefficient
r	Displacement from the source; distance along radius
r_o	Radius of pipe
s	Distance along axis of diffusion
T	Wave period
t	Time
U_A	Wind velocity
U_*	Friction velocity
U_{max}	Maximum velocity
U_s	Surface current velocity
u, v, w	Instantaneous velocities along x, y, z axes, respectively
u', v', w'	Instantaneous velocity fluctuations along x, y, z axes, respectively
$\bar{u},\bar{v},\bar{w}$	Mean velocities along x, y, z axes, respectively
u''	Root mean square of instantaneous velocity fluctuation along x axis
W_1	Weight of diffusant per unit area
W_2	Weight of diffusant per unit length
W_3	Weight of diffusant
x	Coordinate axis in direction of transport

y	Coordinate axis in direction laterally normal to that of transport
z	Coordinate axis in vertical direction
α	Dilution coefficient
β	Temperature correction factor
γ	Energy dissipation parameter
κ	Von Karman's constant
ξ	Time
ρ	Mass density of fluid
ρ_A	Mass density of air
σ	Standard deviation
σ_0	Initial standard deviation
$\sigma_x, \sigma_y, \sigma_z$	Standard deviation along x, y, z axes, respectively
τ	Shear stress
τ_0	Wall shear stress
τ_s	Free surface shear stress
θ	Temperature
θ_s	Standard Temperature
ν	Viscosity
ω	Diffusivity parameter

LIST OF FIGURES

Figure	Title	Page
3-1	Schematic Diagram of Continuous Flow Sampling Apparatus	36
3-2	Continuous Flow Sampling Apparatus	38
3-3	Boat used in Dispersion Tests	38
3-4	Devices used for Simultaneous Collection of Discrete Samples in Vertical	40
3-5	Wave Gage	42
3-6	Drogue for Measuring Currents at Various Depths	42
3-7	Temperature Correction Curve	46
3-8	Calibration Curve for Concentraion of Rhodamine B	47
3-9	Map of Test Sites	52
4-1	Velocity Distribution with Depth	62
4-2	Decrease in Relative Concentration with Time	66
4-3	Dilution Coefficient versus Velocity of Surface Current	74
4-4	Dilution Coefficient versus Velocity of Surface Current Corrected for Surface Conditions	75
4-5	Vertical Concentration Profiles at Various Times	77
4-6	Graphical Determination of Standard Deviation	79

4-7	Vertical Dispersion Coefficient versus Surface Current	82
4-8	Vertical Dispersion Coefficient versus Water Particle Orbital Velocity	83
4-9	Vertical Dispersion Coefficient versus Total Velocity of Water Particle	84
4-10	Vertical Dispersion Coefficient versus Wave Height	86
4-11	Strip Chart of Fluorescence Profile for Lateral Traverse	87
4-12	Method of Estimating Standard Deviation from Fluorescence Profile	89
4-13	Graphical Method of Calculating D_y	90
4-14	Lateral Dispersion Coefficient versus Surface Current Velocity	93
4-15	Relationship between Lateral and Vertical Coefficients of Dispersion	94
4-16	Strip Chart of Fluorescence Profile for Longitudinal Traverse	96
4-17	Concentration Profile in Curving Cloud	97

CHAPTER 1

INTRODUCTION

1-1 General

Most water pollution problems involve diffusion processes. Removal of all pollutants from waste effluents at the point of emission or outfall is seldom practical because of high costs and lack of technical knowledge; therefore, economy demands maximum utilization of the assimilation capacity of the receiving body of water. Efficient use of the natural disposal system requires knowledge of the processes by which the contaminants are mixed and dispersed in the receiving water.

Most of the dispersion studies which have been concerned with water pollution problems have dealt with flowing streams or with tidal bodies. This is natural and proper since most water pollution problems have occurred in rivers and estuaries, but the pollution problem is becoming increasingly important in lakes and reservoirs. Pollution problems in Lake Erie and Lake Tahoe, for example, have received much publicity. Increasing use of lakes for cooling water has made thermal pollution an item of economic concern in many parts of the United States. Man is busily damming up many streams to make reservoirs for power, flood control and water conservation and, in so doing, compounds the problems caused by his ever-increasing rate of waste production.

In lakes, wind-produced currents and waves are often the most important factors influencing the mixing and dispersion process. Wind blowing over the surface of a lake causes a current to develop in the upper layers of the water. At the surface, this current is in the general direction of the wind. The velocity diminishes rapidly with depth and reverses direction somewhere in the cross section to maintain continuity. If the wind velocity is of sufficient magnitude, waves are formed on the water surface. At higher wind velocities, many of the waves break producing high turbulence.

An interchange of fluid between two zones in a turbulent field results in the simultaneous interchange of every characteristic of the fluid masses involved. Envision a fluid mass labeled with a tracer and separated by an imaginary boundary from a fluid mass containing no tracer. To satisfy continuity, a small portion of the marked fluid moved across the boundary must be replaced by an equal volume of unmarked fluid. This results in a decrease in concentration of tracer in the mass on one side of the boundary and an increase in concentration of tracer in the mass on the other. If the process is repeated indefinitely, a uniform concentration of the tracer throughout both zones will eventually result. The masses involved in turbulent exchange are ill-defined lumps of fluid called eddies, and the process is known as eddy diffusion.

Eddy diffusion is considered to be similar to molecular diffusion, the process by which properties migrate through fluids and solids as a

result of Brownian motion of the molecules. The eddies and their random motion are considered analogous to the molecules and their random Brownian movement.

When observing the behavior of a tracer in a receiving water where a velocity gradient exists, one finds an apparent diffusion which is much greater than that accountable through turbulent diffusion alone. This is mainly due to the variation in the convective transport associated with the nonuniform velocity profile. The combined process is referred to as dispersion and is assumed to occur as a result of molecular and turbulent diffusion and as a result of shear flow mixing due to the velocity gradients existing within the body of water.

1-2 Objectives and Scope

The dispersion of pollutants in lakes and reservoirs has only recently come under study. Very little is known of the hydromechanical behavior and transport phenomena in these small impoundments in which the main currents are wind-generated. Before concerted studies of mixing and dispersion phenomena can be undertaken, it is first necessary to be able to define the various factors which affect these phenomena and then to determine whether relationships exist among these various factors.

To date, little data are available from which to determine actual numerical values of dispersion coefficients in lakes and reservoirs. The effects of scale, time diminution of peak concentration, depth of mixing,

etc. are virtually unknown for fresh water impoundments. Therefore, in an effort to help fill this gap, it was the general purpose of the research presented herein to investigate experimentally the mixing and dispersion processes in an actual existing deep water reservoir.

A characteristic of primary interest to engineers is the dilution rate, i. e., the rate at which the peak concentration in a dispersing cloud of pollutant diminishes. One specific objective of this study was to make field measurements of the peak concentration in a dispersing cloud as the concentration diminished with time. The rate will be examined for relationships with the current and wave conditions and will be compared with the various theories which have been developed for its prediction.

The carrying capacity of turbulent eddies, called eddy diffusivity or the coefficient of eddy diffusion, is a characteristic of particular interest to fluid dynamicists concerned with diffusion. In the field, as was noted previously, dispersion may be affected by other processes in addition to molecular and pure turbulent diffusion. The term coefficient of dispersion will be used hereinafter to describe the apparent diffusivity resulting from all dispersion processes which might be acting. A second objective of the study was to develop techniques for making field measurements of concentration profiles in a cloud or plume of dye dispersing in a deep reservoir in order to calculate the coefficients of dispersion.

Coefficients so calculated will be examined qualitatively for effects of scale and for correlation with such factors as surface currents and wave conditions.

This study was limited to Lake Travis (a relatively deep reservoir of medium size), to time scales of less than six hours, and to dye releases at the surface only.

CHAPTER 2

BACKGROUND

2-1 Theoretical Background

Diffusion is the movement of a substance within another (the diffusing phase being in solution or suspension within the dispersing phase) or the migration of some property of the substance, such as its temperature.

Diffusion takes place whenever there is a gradient of the concentration of the dispersed phase or the intensity of the property which migrates. If the dispersing phase is in the solid state, the diffusion takes place as a result of molecular motion; if it is in the fluid state, the diffusion takes place as a result of either the molecular movements alone or the combined effect of molecular motion and the movements of macroscopic masses of the fluid.

The rate of transfer of properties depends fundamentally upon two independent variables: the extent of the difference of the characteristic in question between two adjacent zones (the gradient of concentration or intensity) and the carrying capacity of the flow. The basic equations of diffusion were first given by the physiologist Fick, and have become known as Fick's Laws of Diffusion. Fick's first law is given by the equation:

$$M = -D\frac{dc}{ds} \tag{2-1}$$

in which M represents the rate of transport of the characteristic of intensity or concentration c by diffusion in the direction of s across a unit area normal to s. The negative sign indicates that the transport is in the direction of decreasing concentration. D is a proportionality constant called the diffusion coefficient or diffusivity and corresponds to the carrying capacity of the flow as noted above.

As an example, if the flow characteristic in question is the momentum of the fluid, the basic diffusion equation leads to the shear equation (for laminar flow):

$$\tau = \nu \frac{d(\rho u)}{dz} \tag{2-2}$$

The negative sign has disappeared as a result of the directional sense arbitarily assigned to the shear stress,

Combining equation (2-1) with the law of conservation of mass leads to Fick's Second Law of Diffusion:

$$\frac{\partial c}{\partial t} = D\frac{\partial^2 c}{\partial s^2} \tag{2-3}$$

The coefficient of diffusion, D, represents both physically and dimensionally the combination of a length and a velocity which together characterize the nature of the diffusion process. Einstein, in a theory of Brownian motion, defined the diffusion coefficient by

the differential equation:

$$D = \frac{1}{2} \frac{d(\sigma^2)}{dt} \qquad (2\text{-}4)$$

This equation assumes that the random molecular motion causes normal distribution of the diffused substance or property. σ is the standard deviation. The equation is not restricted to those cases in which the diffusion coefficient is constant.

In a turbulent flow regime, the diffusion that results from the macroscopic turbulent movements of the fluid is known as turbulent or eddy diffusion. While the process is not truly one of diffusion in the classical sense, a strong analogy exists between the behavior of fluid masses and the nature of molecular motion. In other words, the eddies which are characteristic of turbulent flow are assumed to exhibit a random type of motion which is similar to molecular motion, and the differential equations which describe the two motions are assumed to be similar. Thus equations (2-1) and (2-3) are applied to both molecular and eddy diffusion by use of appropriate values of D.

The values of the coefficient of molecular diffusion vary with the substances involved and with the temperature. Under most conditions molecular diffusion is isotropic and the diffusion coefficient is constant. A simple constant, D, cannot be established to define turbulent diffusion, however, because the turbulent diffusion process

depends upon the turbulent structure of the flow. Since the turbulence is usually non-isotropic, the turbulent diffusion coefficient may be a function of space. It may vary with the scale of the turbulence and is normally many orders of magnitude larger than the molecular diffusion coefficient.

Equation (2-3) is for the case of one dimensional diffusion with a constant value of D. For the more general three dimensional case with variable and non-isotropic diffusivity, the equation becomes:

$$\frac{\partial c}{\partial t} = \frac{\partial}{\partial x}\left(D_x \frac{\partial c}{\partial x}\right) + \frac{\partial}{\partial y}\left(D_y \frac{\partial c}{\partial y}\right) + \frac{\partial}{\partial z}\left(D_z \frac{\partial c}{\partial z}\right) \qquad (2\text{-}5)$$

By analogy with the kinetic theory of gases Prandtl postulated that as the masses of fluid migrated laterally they carried with them the mean velocity (and hence the momentum concentration) of their point of origin. Thus if the flow is two dimensional with a velocity $\bar{u}(z)$ in the direction of x, a typical velocity fluctuation u' caused by a migration can be characterized as:

$$u' = \ell \frac{d\bar{u}}{dz} \qquad (2\text{-}6)$$

where l, the so-called mixing length, is the distance over which a migration takes place. The mixing length is related to the mean free path of parcels of fluid and is analogous to the mean free path of molecules within the system.

If the vertical velocity fluctuation, w', is considered to be proportional to the horizontal velocity fluctuation, u', and the turbulent shear, τ, proportional to the product of $\overline{u'w'}$, then:

$$\tau = \rho l^2 \left|\frac{d\bar{u}}{dz}\right| \frac{d\bar{u}}{dz} \qquad (2\text{-}7)$$

where l has absorbed the coefficients of proportionality. The absolute value of the velocity gradient is used so that the signs of τ and the gradient will be in order.

The advantage of Prandtl's approach is that the variable involved is simply a length, enabling a more plausible explanation for l than that for D which is the product of a length and a velocity. In fact, the mixing length concept can be considered as an assumption regarding the makeup of D:

$$D = l^2 \left|\frac{d\bar{u}}{dz}\right| \qquad (2\text{-}8)$$

Von Karman (1930) attempted to relate the turbulence characteristics to the mean velocity characteristics alone. Similarly to Prandtl, he assumed the turbulent fluctuations to be proportional to a length, l, and the mean velocity gradient, $\frac{d\bar{u}}{dz}$, and the intensity of shear to be $\rho l^2 \left(\frac{d\bar{u}}{dz}\right)^2$. The length l, however, was considered to be proportional to $\frac{d\bar{u}}{dz}$ divided by $\frac{d^2\bar{u}}{dz^2}$:

$$\sqrt{\frac{\tau}{\rho}} = -\chi \frac{\left(\frac{d\bar{u}}{dz}\right)^2}{\frac{d^2\bar{u}}{dz^2}} \qquad (2\text{-}9)$$

where χ is a universal constant having a value estimated to be about 0.4.

These concepts relate the turbulent structure at a point to the mean velocity structure at the same point instead of to an area of influence, an oversimplification of the process.

Richardson (1926) developed another type of diffusion equation by relating the average separation of particle pairs projected on an arbitrary axis, l. He assumed that the important independent variable in turbulent diffusion is separation of the particles of the diffusant rather than the actual particle position. His equation is:

$$\frac{\partial q}{\partial t} = \frac{\partial}{\partial l}\left[F(l)\frac{\partial q}{\partial l}\right] \qquad (2\text{-}10)$$

where q is the mean number of diffusing particles (neighbors) per unit length, and F(l), the neighbor diffusivity, is analogous to the diffusion coefficient and is a function of the particle separation, l. Since l is in effect a measure of the areal extent of the diffused substance, F(l) is dependent on the scale of the diffusion phenomenon.

Richardson concluded from some measurements on smoke plumes that:

$$F(\ell) \sim \ell^{4/3} \tag{2-11}$$

It is to be noted that if the diffusion is Fickian (i. e. if $F(l) = D$ and is constant) Richardson's equation is identical to equation (2-3).

$$\frac{\partial q}{\partial t} = D \frac{\partial^2 q}{\partial \ell^2}$$

Kolmogoroff (1941) theorized that for large Reynolds numbers, the rate of diffusion should be a function of the 4/3 power of the scale of the turbulence times the 1/3 power of the rate of energy dissipation per unit mass of fluid. He reasoned that for flows with large Reynolds numbers, energy from the larger eddies is transferred down through the spectrum to the smaller eddies, where it is finally dissipated through viscous action. In the larger eddies, a relatively small proportion of the energy is dissipated by viscosity and virtually all is transferred to the smaller eddies. As the eddy size decreases, a larger portion of the energy is dissipated by viscous action until the role of viscosity becomes significant. Kolmogoroff hypothesized that there is a subrange in the spectrum in which the eddies are isotropic and where the statistical characteristics of the turbulence are governed by both the viscosity and the rate of energy transference. Assuming that an analogy exists between molecular and turbulent diffusion so that the viscosity can be replaced by a turbulent diffusion coefficient, dimensional analysis gives the relation:

$$D \sim \ell^{4/3} E^{1/3} \qquad (2\text{-}12)$$

When E (the rate of energy dissipation per unit mass through turbulence) is constant, this equation is of the same form as Richardson's equation of a "four-thirds law" (2-11).

G. I. Taylor (1921) made the first thoughtful application of statistical concepts to turbulence theory. His theory was built around statistical correlation of fluid particle velocities at points in the fluid stream separated by a time interval. He arrived at a Lagrangian correlation coefficient, $R(\xi)$, which is a correlation between the fluctuation component of the velocity at time t and again at time $t + \xi$:

$$R(\xi) = \frac{\overline{u'(t)\, u'(t+\xi)}}{\sqrt{\overline{u'(t)}^2}\,\sqrt{\overline{u'(t+\xi)}^2}} \qquad (2\text{-}13)$$

As ξ increases, there is less correlation between $u'(t)$ and $u'(t+\xi)$. The value of $R(\xi)$ varies from unity when ξ is zero and approaches zero when ξ becomes very large.

A corresponding Eulerian correlation coefficient is more easily obtained by substituting distance for time. Ippen and Raichlen (1957) have measured the Eulerian function in open channels. Orlob's (1959) experiments indicate that the Eulerian correlation function gives a reasonable estimate of the Lagrangian function.

For small values of time, ξ :

$$R(\xi) = 1$$

$$\int_0^t d\xi = t$$

$$\chi = \bar{u} t$$

The pattern of diffusion immediately after release is wedge-shaped. For times greater than, t_o, the time required for zero correlation, the value of the integral is constant:

$$D = \bar{u}^2 \int_0^{t \geq t_o} R(\xi) d\xi \qquad (2\text{-}14)$$

Thus the pattern of diffusion is parabolic for $t \geq t_o$. Between these values, Ippen and Raichlen have found the correlation coefficient can be approximated by the form $R(\xi) = e^{-N}$ giving an easily integrated expression

$$\int_0^{t < t_o} R(\xi) d\xi = \frac{1 - e^{-Nt}}{N} \qquad (2\text{-}15)$$

And the pattern of diffusion is

$$\sigma = 2\left(\frac{\bar{u}}{N}\right)^2 (Nt - 1 + e^{-Nt}) \qquad (2\text{-}16)$$

Batchelor (1952), with the aid of dimensional arguments and ergodic hypothesis, finds three regimes of relative diffusion. If the initial size of the cloud is small, these regimes are characterized by the following rates of growth:

(1) Initial

$$\frac{d(\sigma_x^2)}{dt} = k_1 t (E\sigma_0)^{2/3} \qquad (2\text{-}17a)$$

(2) Intermediate

$$\frac{d(\sigma_x^2)}{dt} = k_2 E (t - t_1) \qquad (2\text{-}17b)$$

where

$$t_1 = k_3 \sigma_0^{2/3} E^{-1/3} \qquad (2\text{-}17c)$$

(3) Asymptotic

$$\frac{d(\sigma_x^2)}{dt} = k_4 u'' l \qquad (2\text{-}17d)$$

k_1 to k_4 are constants of order unity, σ_x is the standard deviation measured along x, t is time, σ_o is the initial standard deviation of the cloud, and E is the rate of energy dissipation per unit mass through turbulence. For E an additional relationship may be noted:

$$E = \frac{(u'')^3}{l} \qquad (2\text{-}18)$$

with u'' the root mean square turbulent velocity along the x axis and l the scale of turbulence. By analogy with molecular diffusion an equivalent diffusivity may be introduced by the relationship expressed in equation (2-4). From equations (2-17) it is seen that the diffusivity is constant in the final phase, while it grows as the 4/3 power of cloud size in the intermediate phase as noted in Richardson's law of relative diffusion. Relative diffusion is thus an accelerating process, the rate of growth increasing with the size of the cloud while the supply of eddies of requisite size lasts. When the cloud becomes large compared with the typical eddy in the diffusing field, its growth rate becomes constant and resembles molecular diffusion except that the magnitude of diffusivity is of a higher order of magnitude.

Csanady (1963) applied Batchelor's formulae to horizontal dispersion in a lake by introducing a "gustiness" term as the ratio of the root mean square of the turbulent component of the surface current to the mean velocity of the surface current

$$g_x = \frac{u''}{\bar{u}} \tag{2-19}$$

and transforming the time coordinate into distance drifted by

$$x = \bar{u} t$$

to arrive at the following equations

Initial

$$\frac{d(\sigma_x^2)}{dx} = k_1 \times g_x \left(\frac{\sigma_0}{\ell}\right)^{2/3} \tag{2-20a}$$

Intermediate

$$\frac{d(\sigma_x^2)}{dx} = k_2 \times g_x^2 \left(\frac{x}{\ell}\right) \tag{2-20b}$$

Final

$$\frac{d(\sigma_x^2)}{dx} = k_4 g_x \ell \tag{2-20c}$$

Csanady reported that in regular diffusion the three phases predicted by the theory are easily recognizable in spite of the expected statistical scatter. The two dispersion constants g_x and l were extracted from the data by estimating the slope, $\frac{d(\sigma_x^2)}{dx}$, in the intermediate

and final phases. Assuming the constants k_2 and k_4 to be unity, the asymptotic value of the diffusivity is given by intergrating equation (2-20c):

$$D = \frac{1}{2} g_x \ell \bar{u} \qquad (2\text{-}21)$$

The most nearly complete and satisfactory analysis with respect to shear flow mixing has been made by Taylor (1954) for pipe flow. In this analysis the universal velocity distribution law, credited to Von Karman, was combined with the Reynolds analogy. The universal velocity distribution law is:

$$\frac{u_{max} - u}{\sqrt{\tau_0/\rho}} = f\left(\frac{r}{r_0}\right) \qquad (2\text{-}22)$$

where u_{max} is the maximum velocity (centerline), u is the velocity at any point of distance r from the center of the pipe of radius r_o. τ_0 is a wall shear and ρ is the mass density of the fluid. The Reynolds analogy is:

$$\frac{\tau}{\rho \frac{\partial u}{\partial r}} = \frac{M}{\frac{\partial c}{\partial r}} \qquad (2\text{-}23)$$

This relationship states that momentum transfer equals diffusant transfer where τ is the shear at any point in the fluid, $\frac{\partial u}{\partial r}$ is the velocity gradient at the point, M is the mass rate of transfer of diffusant at the point and $\frac{\partial c}{\partial r}$ is the concentration gradient at the point.

Through a complicated analysis, Taylor derived the formula

$$D_x = 10.1 r_o u_* \qquad (2\text{-}24)$$

in which $u_* = \sqrt{\tau_o/\rho}$ is the friction velocity and D_x is the longitudinal dispersion coefficient. Taylor named D_x the virtual diffusion coefficient because it fits a solution of the diffusion equation. The constant 10.1 is made up of 10.05 from shear flow mixing and 0.05 from turbulent diffusion. The 0.05 from turbulent diffusion was obtained by assuming the longitudinal and transverse turbulent diffusion to be equal (isotropic turbulence).

Using a similar analysis, Elder (1959) found the effective longitudinal dispersion coefficient, D_x, in a broad open channel to be:

$$D_x = 5.9 u_* h \qquad (2\text{-}25)$$

where U_* is the friction velocity based on the shear stress at the bottom of the channel of depth h. To adapt this equation to a wind-driven lake current, Csanady (1963) formed the friction velocity from the shear stress on the surface. To obtain the surface shear stress, τ_s, he used the relationship developed by Deacon (1962):

$$\tau_s = 0.0012 \rho_A U_A^2 \qquad (2\text{-}26)$$

where ρ_A is air density and U_A is the wind velocity at the 10 meter level. The friction velocity is then

$$U_* = \sqrt{\tau_s/\rho} = U_A\sqrt{0.0012\,\rho_A/\rho} \qquad (2\text{-}27)$$

and the longitudinal dispersion coefficient is:

$$D_x = 5.9\,h\,U_A\sqrt{0.0012\,\rho_A/\rho} \qquad (2\text{-}28)$$

Equation (2-3), Fick's Second Law of Diffusion, is the fundamental equation for dispersion of a fluid property in a one dimensional case with constant diffusion coefficient and no advection. If the fluid is moving with an average velocity, $\bar{u}$, the equation becomes

$$\frac{\partial c}{\partial t} = D_x\frac{\partial^2 c}{\partial x^2} - \bar{u}\frac{\partial c}{\partial x} \qquad (2\text{-}29)$$

Diachishin (1963) presents a solution to this equation for a slug input at a point source in a fluid of infinite extent:

$$c = \frac{W_1}{\sigma_x\sqrt{2\pi}}\exp\left[-\frac{1}{2}\left(\frac{x-\bar{u}t}{\sigma_x}\right)^2\right] \qquad (2\text{-}30)$$

where W_1 is the weight of dye in the cloud per unit area.

Several interesting methods for finding the value of D_x are also presented by Diachishin. The first, credited to Krenkel and Orlob, in-

volves plotting the logarithm of $ct^{1/2}$ vs. $(x - \bar{u}t)^2/t$. The slope of the line is equal to $4D_x$. This can be verified by taking logarithms of both sides of equation (2-30) after making the substitution $\sigma_x = \sqrt{2D_x t}$.

Another method is very similar except that the measurements of concentration at various times are made very near the source. Thus x is very small and may be neglected. Then log $ct^{1/2}$ is plotted against t and the slope of the line is again $4D_x$.

In a third method, the equation $\sigma_x = \sqrt{2D_x t}$ is used. A plot of σ_x vs. $t^{1/2}$ will give a straight line through the origin with a slope of $\sqrt{2D_x}$.

Diachishin also presents a two-dimensional solution of the Fickian diffusion equation:

$$C = \frac{W_2}{2\pi\sigma_x\sigma_y} \exp\left[-\frac{1}{2}\left(\frac{x-\bar{u}t}{\sigma_x}\right)^2 - \frac{1}{2}\left(\frac{y-\bar{v}t}{\sigma_y}\right)\right] \quad (2\text{-}31)$$

where W_2 is the weight of dye per unit length.

The three-dimensional solution is:

$$C = \frac{W_3}{(2\pi)^{3/2}\sigma_x\sigma_y\sigma_z} \exp\left[-\frac{1}{2}\left(\frac{x-\bar{u}t}{\sigma_x}\right)^2 - \frac{1}{2}\left(\frac{y-\bar{v}t}{\sigma_y}\right)^2 - \frac{1}{2}\left(\frac{z-\bar{w}t}{\sigma_z}\right)^2\right] \quad (2\text{-}32)$$

where W_3 is the total weight of dye in the cloud. The maximum concentration in the three-dimensional case is at the center of the dye mass and is:

$$C_{MAX} = \frac{W_3}{(2\pi)^{3/2}\sigma_x\sigma_y\sigma_z} \qquad (2\text{-}33)$$

and since $\sigma = \sqrt{2Dt}$

$$C_{MAX} = \frac{W_3}{8\pi^{3/2} D_x^{1/2} D_y^{1/2} D_z^{1/2} t^{3/2}} \qquad (2\text{-}34)$$

So that the maximum concentration is inversely proportional to the 3/2 power of the time elapsed from the time of release.

Many investigations, including a theoretical study by Batchelor (1952), and an empirical model study by Orlob (1959), have provided some support for Richardson's (1926) law that the coefficient of eddy diffusivity is proportional to the 4/3 power of the scale of the disturbance near the source.

Based on an empirical study in the field, Parker (1961) concluded that the diffusivity varied as a power function of the eddy radius. It is possible, however, that the coefficient becomes constant after some distance of travel. If turbulence is considered to be a superposition of eddies of all sizes, then it would seem likely that the diffusion coefficient would increase with the size of the patch until the patch reached the size of the largest eddy and thereafter remain constant. The effect of the eddies larger than the patch is obviously convection which would

move the whole patch with no effect on its shape or size. The diffusion within the patch is influenced by those eddies of the scale equal to or less than the size of the patch. In the ocean, of course, the eddies can be very large and for engineering purposes the mixing can perhaps be assumed to follow the four-thirds law.

Okubo (1962), in a survey of theoretical models for turbulent diffusion in the sea, reviews and compares several solutions for the time and space distributions of mean concentration from an instantaneous vertical line source in an ocean of infinite horizontal extent. The predictions for peak concentration vs. time and the assumptions upon which each derivation was based are:

(1) Joseph and Sendner (1958) assumed that diffusivity varies with the distance from the center of the cloud:

$$C_{MAX} = \frac{W_2}{2\pi p_1^2} t^{-2} \qquad (2\text{-}35)$$

p = diffusion velocity (cm / sec)

(2) Ozmidov (1958) assumed that diffusivity varies with the 4/3 power of the distance from the center of the cloud:

$$C_{MAX} = \frac{W_2}{6\pi \gamma_1^3} t^{-3} \qquad (2\text{-}36)$$

γ = energy dissipation parameter ($cm^{2/3}$ / sec)

(3) Okubo and Pritchard assumed that diffusivity varies with time:

$$C_{MAX} = \frac{W_2}{\pi P_2^2} t^{-2} \qquad (2\text{-}37)$$

(4) Okubo assumed that diffusivity varies with time and with the 2/3 power of the distance from the center of the cloud:

$$C_{MAX} = \frac{W_2}{\frac{3}{4}\pi^{3/2}\gamma_2^3} t^{-3} \qquad (2\text{-}38)$$

(5) Obukhov (1959) assumed that diffusivity varies with time squared:

$$C_{MAX} = \frac{W_2}{\pi \gamma_3^3} t^{-3} \qquad (2\text{-}39)$$

(6) Schonfeld (1959) introduced a concept called integral diffusion and assumed that the scale of the turbulence varies linearly:

$$C_{MAX} = \frac{W_2}{2\pi P_3^2} t^{-2} \qquad (2\text{-}40)$$

The Fickian solution, assuming isotropic diffusion, is:

$$C_{MAX} = \frac{W_2}{4\pi D} t^{-1} \qquad (2\text{-}41)$$

For spatial distribution of concentration, Okubo finds his solution to be "a little superior to the others" but he does not comment on the best relationship for the peak concentration.

2-2 Previous Experimental Efforts

Since the values obtained by the investigators for the eddy

diffusion coefficients have varied so widely, it has occurred to some that there might be a correlation between the diffusivity and ambient conditions. Cramer (1959) reported that atmospheric dispersal capacity can be predicted with reasonable accuracy from its correlation with the mean wind speed and the frequency distribution of azimuthal wind direction under given conditions of stability. Stommel and Woodcock(1951) attempted to correlate eddy diffusivity in the surface of the ocean with wind strength but met with little success. Wiegel (1964) suggests that the eddy diffusivity is related more closely to the wave spectrum generated by the wind than to the wind itself. Masch (1961; 1962) in studying the effect of wind waves on the dispersion of floating polyethelene spheres in a tank, found that except near the source, D_y was essentially a constant which correlated with the sum of the surface current and the water particle orbit speed. Because of close correlation between significant wave conditions and the maximum energy in the wave spectrum, these results support the spectrum idea rather than wind alone. Katz, et al(1965) analyzing aerial photographs of a number of sea surface dye tracer experiments, found a strong correlation among wind, sea state, and the development of the patch of dye. In general they found that as the wind velocity and sea state increase, the rate of elongation decreases and the depth of penetration increases. They concluded that the spreading of a contaminant at the sea surface is not a wholly random process but is strongly influenced by ambient condtions.

Ichiye (1962), from experiments in the Gulf of Mexico, concluded that dye patches generally diffuse more intensely along the direction of the wind. He found that the clouds were elongated and/or broken into pieces for wind speeds greater than 3 meters per second or for surface currents greater than 10 centimeters per second. He noted that in a condition of strong wind and weak current the patch tended to elongate in the direction of the wind, but that the elongation was in a lateral direction when the current was strong and the wind weak.

Foxworthy, et al (1966), in a series of experiments in the Pacific Ocean, found that the maximum concentration in a dye plume was a function of the distance from the source raised to a power ranging from 0.98 to 1.85. They also reported that the lateral variance of the concentration distribution was a function of the distance raised to a power ranging from 0.92 to 2.24. It must be noted that the summary of oceanographic conditions existing during the tests indicates that the dye transport velocity and direction were not related to wind velocity and direction. As in almost all investigations reported in the literature, the currents in the water were not primarily wind-generated.

Bowden (1964) found that the effective coefficient of horizontal dispersion in the sea is inversely proportional to the coefficient of vertical eddy diffusion. In a shearing current the vertical gradient of velocity combined with vertical turbulent mixing leads to an effective

dispersion in the horizontal direction. Good vertical mixing reduces the concentration gradients and thus counteracts the tendency for a cloud to be sheared according to the velocity profile. If there is little vertical mixing, differential horizontal transport occurs at the various levels by virture of the larger velocity differential which exists. Vertical diffusion acts to spread out in the vertical the material convected at one height. The occurrence of a stable density gradient which inhibits vertical mixing, therefore, increases the effective horizontal mixing very considerably.

In atmospheric dispersion studies, Saffman (1962) with an analytical approach and Pasquill (1962) using an experimental technique both found that if the atmosphere is bounded at a finite height, the horizontal spread is inversely proportional to the vertical transport. For diffusion in the atmosphere, the vertical eddy diffusivity will, in general, be relatively small near the ground so that the wind profile at lower levels may have more influence on the spread of the cloud than does the profile at higher levels. Similarly, Bowden found that the vertical eddy diffusivity in an estuary was lowest near the surface, reached a maximum near mid-depth and then decreased toward the bottom. The horizontal diffusivity behaved in the opposite manner and thus appears to be a function of depth.

Csanady (1963) studied the dispersion of small floating objects and of fluorescent dye in Lake Huron. He reported that the dispersal of

floating objects exhibited an increase in rate of growth with the size of the diffusing cloud but had no relationship to meteorologic conditions. Along the direction of the current the diffusion of dye was found to be accelerated by the changes of current velocity with depth much as in a pipe or channel. Csanady (1966) reported that apparent horizontal diffusivities increase steeply in complex currents because the horizontal diffusion is accelerated by directional change of velocity with depth.

CHAPTER 3

EQUIPMENT AND TECHNIQUES

To examine the dispersal characteristics of a body of water, it is essential to observe the rates of change of concentration of a property of the water with respect to time and distance. The concentration of the fluid property must, of course, be readily measurable. If there is no naturally occurring characteristic which can be used as the measured diffusing property, an artificial tracer must be added. Naturally occurring properties which are used in dispersion studies include salinity and temperature. Floats, dyes, and radioisotopes are among the most common artificial tracers used in studies of dispersion in water.

In this experimental investigation a dye was used as the tracer. A fluorescing dye was chosen so that its concentration could be measured with a fluorometer. The following sections will describe the dye selected, the fluorometer and other equipment used, as well as the techniques employed.

3-1 Tracer

The ideal tracer for turbulent diffusion measurements should have the same specific gravity, viscosity, and other physical and chemical characteristics as the water in which it is dispersed so that it responds perfectly to the movement of the water and to the random move-

ments which lead to turbulent dispersion. It must be sensitively and easily detected quantitatively, easily resolved from naturally occurring substances, cheap, easy to handle, and offer no hazard to man or to aquatic life.

Rhodamine B, a commercial organic pigment, is an excellent tracer material. It is available commercially in a 40% by weight solution in acetic acid. The current cost is approximately $2.00 per pound of solution. Rhodamine B is non-toxic, quite soluble in water and highly soluble in methanol so that concentrated solutions may be adjusted to the same density as the receiving water. It is easily detected by its fluorescence. The absorption spectrum of Rhodamine B peaks at approximately 550 millimicrons so that the molecule is readily excited by the green (546 millimicron) line of mercury. Its fluorescence spectrum is a maximum at approximately 580 millimicrons and extends into the red portion of the spectrum. Naturally occurring fluorescent substances are excited by shorter wavelengths and also emit light of shorter wavelength. Thus by proper selection of the primary and secondary filters used in a fluorometer, interference of naturally occurring substances with the fluorescence of Rhodamine B is minimized.

Rhodamine B is not seriously affected by light or bacterial action. The most significant enviromental influence on the fluorescence of Rhodamine B is temperature. Pritchard and Carpenter

(1960), pioneers in the use of the fluorometer in field studies of dispersion, found that the fluorescence decreases with increasing temperature at the rate of 2.3% per degree centigrade. Feuerstein and Selleck (1963) found the response to temperature change to be:

$$F_s = F e^{-0.027(\theta_s - \theta)} \qquad (3\text{-}1)$$

where F_s is the fluorescence reading at θ_s, the standard temperature; and F is the fluorescence reading at θ, the sample temperature. The fluorescence varies so greatly with temperature that sample temperature must be monitored for accurate determinations of concentration.

3-2 Fluorometer

The instrument used to detect the concentration of tracer dye in these dispersion studies is the Turner Model 111 Fluorometer. The fluorometer is basically an optical bridge (analogous to the Wheatstone bridge used to measure electrical resistance) in which the light emitted by the sample is balanced with light from calibrated rear light path. One leg of the bridge consists of light from an ultraviolet lamp filtered to a narrow wavelength and passed through the sample exciting the tracer dye to fluoresce. The light emitted from the sample is filtered to pass only the fluorescent wavelengths and is allowed to strike the photoelectric cell. The other leg consists of light from the same ultraviolet lamp passed through a calibrated attenuating device to strike the photoelectric

cell. A servomechanism automatically balances the two legs of the optical bridge by increasing or decreasing the amount of light in the rear light path through manipulation of the attenuating device. A dial connected to the attenuating device then displays the fluorescent reading.

The instrument is fairly rugged and compact and is well-suited to field work when powered by a portable generator or battery convertor. It is insensitive to line voltage fluctuations because the light in both legs of the optical bridge comes from the same ultraviolet lamp source.

The fluorometer may be equipped with a variety of sample doors. The two types used in this work were the high precision discrete sample cuvette and the 20 ml. continuous flow cuvette. Since the fluorescence of the tracer dye used is virtually an instantaneous phenomenon (on the order of 10^{-8} seconds), the flow rate is limited by the maximum allowable operating pressure of the continuous flow door (10 psi). Flows of approximately 2 gpm were used in this investigation.

The fluorometer has four operating ranges to provide a large range of sensitivity. Each range is defined by the size of the aperture emitting light to the sample. The range may be further extended by adding filters. The dial which reports the fluorescence of the sample is calibrated in divisions from 0 to 100. Since the concentration of dye in the sample is directly related to the amount of fluorescence, the machine is calibrated by obtaining dial readings from samples of

known concentration. The dial reading may also be transmitted to a recorder to provide a continuous record of the fluorescence reading.

Fluorescence is the emission of radiation from a molecule or atom following absorption of radiation. From an analytical standpoint, the intensity of fluorescent light emitted by the sample under constant input light intensity is directly proportional to the concentration of the fluorescent compound. Various investigators have agreed with the manufacturer that at low concentrations of the fluorescent material, the response of the fluorometer is linear with the concentration of Rhodamine B tracer. The Operating and Service Manual (1964) provided by the manufacturer lists three reasons for deviation from linearity:

(1) Extremely high concentrations of the fluorescent material, leading to self-absorption of light. This concentration-quenching effect frequently occurs at concentrations above 1 ppm.

(2) High concentrations of a material in the reagents which absorbs either the exciting ultraviolet light or the emitted light.

(3) Non-linearity in a chemical reaction which is used to convert the unknown to a fluorescent material, or non-linear recoveries.

None of these reasons were applicable in this experiment.

Feuerstein and Selleck (1963) reported that the response of Rhodamine B is not linear in the Turner Model 111 fluorometer, but has the relationship:

$$c = kF^n \qquad (3\text{-}2)$$

To overcome problems of non-linearity in the experiment reported herein, the instrument was calibrated by preparing curves of dial reading vs. concentrations of Rhodamine B in lake water. A curve was prepared for each of the four sensitivity ranges. This calibration work agreed with the findings of Feuerstein and Selleck in that the calibration curves were of the same form as equation (3-2).

One problem encountered in using the fluorometer to sample continuously from a moving boat was that of air bubbles. Air bubbles in the cuvette are disasterous to the measurement, and extreme care must be exercised to prevent air entrainment.

Another problem encountered when working in an open boat was light leakage into the fluorometer. It was discovered that the machine would not operate properly in direct sunlight and must be covered. Two other instruments of the same model were borrowed and tested in order to determine whether the problem of light leakage was unique to the fluorometer assigned to the project. The other two

instruments exhibited a similar erratic behavior in direct sunlight. A canvas cover supported by a metal frame was used to shield the fluorometer from the sun's rays.

When using the discrete sample cuvette, readings must be made quickly. The heat generated by the instrument raises the temperature of the sample and causes the fluorescence to decrease as mentioned above. In one test, with room and sample temperature of 75° F, the reading decreased 30% in 15 minutes as the heat of the instrument caused the sample temperature to increase to 98°F.

To correct for the temperature dependence of the Rhodamine B tracer when the continuous flow cuvette was used, the temperature of the water leaving the fluorometer was monitored continuously and recorded along with the fluorescence reading on a strip chart.

3-3 Arrangement of Equipment for Continuous Sampling

Figure 3-1 is a schematic diagram of the continuous flow sampling apparatus which is pictured in figure 3-2. Electrical power was supplied by a 1250 watt, 115 volt, 60 cycle alternator driven by a 3.5 horsepower gasoline engine.

A Jabsco model B3M6 pump provided a flow of approximately 2 gallons per minute through the system. A faucet was provided in the line as a bypass to permit reduction of the flow rate through the fluorometer door without reducing intake flow and response time. The

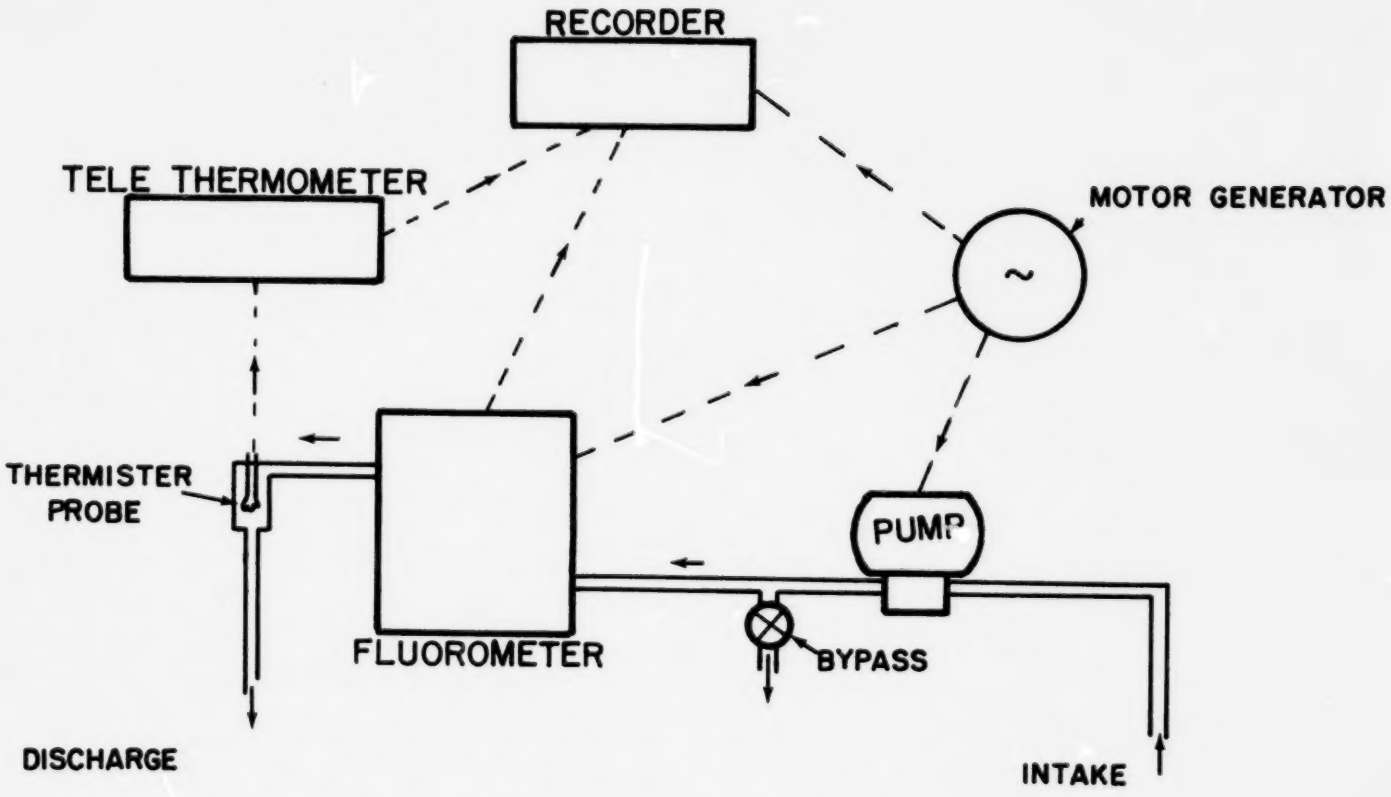

Fig. 3-1 -Schematic Diagram Of Continuous Flow Sampling Apparatus

faucet also facilitated the taking of discrete samples for analysis. Locating the fluorometer on the discharge side of the pump gave no air entrainment problems and proved most satisfactory. One-half inch plastic garden hose was used for all connections.

To measure the temperature of the water at the same time that its fluorescence was being measured, a Yellow Springs Instrument Company model 410 thermistor probe was installed in the fluorometer discharge pipe and connected to a battery powered Yellow Springs Instrument Company model 43 TD tele-thermometer.

Responses from the fluorometer and the tele-thermometer were fed to a YSI model 81 dual channel recorder and recorded on a strip chart. The chart speed was 30 inches per hour.

It might be noted here that a much faster chart speed is highly desirable for use in recording the fluorescence profile measured by traveling through the cloud. At low speeds the chart scale is too small for accurate measurements of time of travel. A chart speed on the order of 3 to 5 inches per minute would be preferable. Because the temperature variations encountered while traveling with the intake at a constant level were insignificant, a single channel recorder is adequate for horizontal measurements.

All of the equipment was mounted on a sheet of plywood (on springs and rubber bushings to reduce vibration) and placed on the deck of the boat.

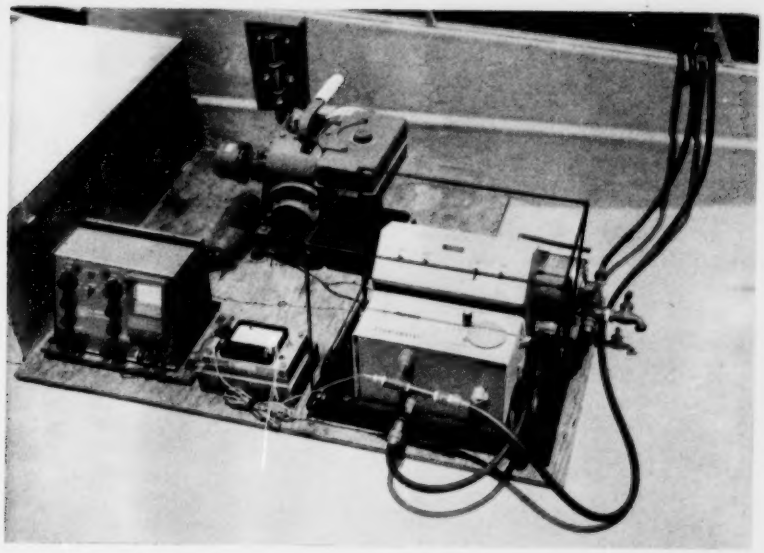

Fig. 3-2 Continuous Flow Sampling Apparatus

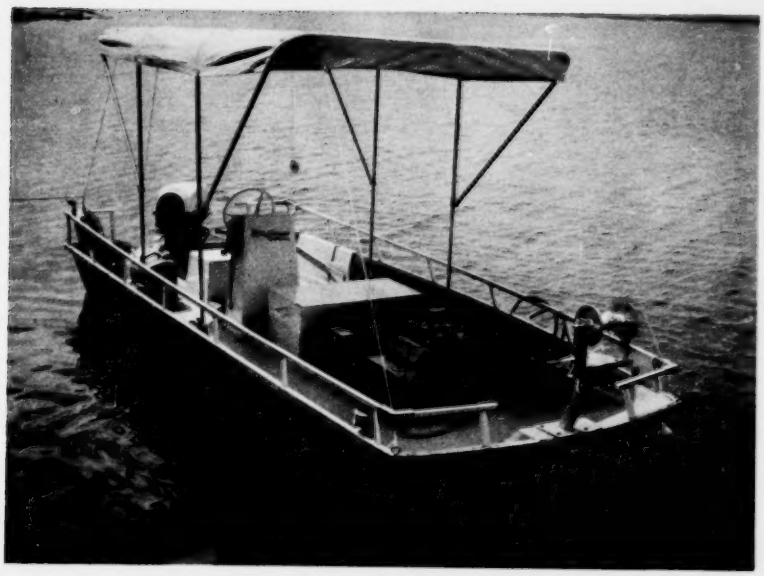

Fig. 3-3 Boat Used In Dispersion Tests

The boat used was a Kenner Ski Barge, pictured in figure 3-3. The broad beam gives the boat excellent stability as well as a large work area, and the flat deck makes the area completely usable. The boat was powered by a 33 horsepower Evinrude outboard motor.

3-4 Discrete Vertical Sampling Device

It proved impossible to hold the boat in a fixed position relative to the dye cloud while a vertical profile of concentration was made with the continuous flow apparatus. It was necessary, therefore, to develop a device capable of taking discrete samples at various depths simultaneously. The samplers devised are pictured in figure 3-4. The samplers were battery syringes fitted with plastic tubing which could be closed with a spring clip. For depths less than ten feet, the syringes were attached at intervals of one foot to a 2" x 2" piece of lumber nine feet long. For deeper sampling, the syringes were connected by snaps to rings spaced five feet apart on a rope. The lower end of the rope was connected to a concrete weight. To collect a sample at each of several depths simultaneously, the syringe bulbs were evacuated of air, and the plastic tubing was closed with spring clips. A line was connected to all of the clips and, after lowering the samplers to the desired depths, the line was pulled to remove the clips and permit the water to fill the bulbs. These devices were used very successfully to depths of fifty feet. The water samples were transferred from the bulbs to plastic bottles and

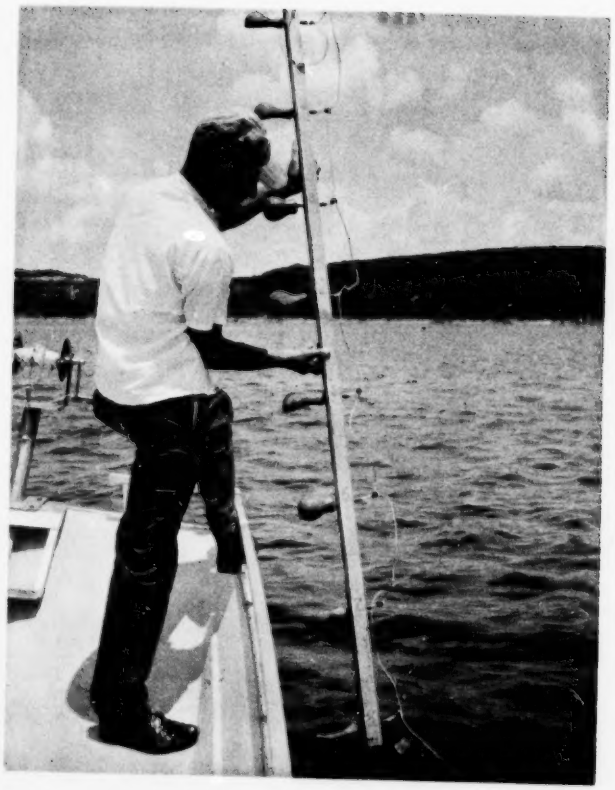

(a) SHALLOW SAMPLER

(b) DEEP SAMPLER

Fig. 3-4 Devices Used For Simultaneous Collection Of Discrete Samples Along Vertical Line

stored until the fluorescence reading could be made. Tests of water samples stored in polyethylene plastic bottles showed no change in fluorescence reading (after temperature correction) during storage periods of twenty-four hours.

3-5 Wave Gage

To estimate wave height and period in the deep waters of the lake, a wave gage (figure 3-5) was made. A piece of 2" x 2" wooden rod ten feet long was graduated in inches. The lower end was attached to a cube of styrofoam and to a steel weight with a three foot length of nylon line. The styrofoam was trimmed until the rod floated in still water with approximately one foot of the gage protruding above the surface. This placed the center of gravity and the center of buoyancy approximately twelve feet below the surface of the water and below the zone of appreciable wave motion for the range of waves encountered in the tests. During the tests, this gage proved to be very stable with virtually no vertical movement.

In use, the gage was anchored near the test area. Wave heights were estimated by noting during the passage of a wave the gage readings of the crest and of the succeeding trough. The difference between the two readings was the wave height. Waves passing the gage were observed for approximately five minutes before, after, and several times during each test. The average wave height determined from these

Fig. 3-5 Wave Gage

Fig. 3-6 Drogue For Measuring Currents

visual observations should be near the significant wave height which is defined as the average of the highest one-third of the waves.

While one observer was estimating the wave height, another was estimating the wave period. The wave period was estimated by repeatedly timing the passage of ten successive crests and calculating the mean of ten such measurements. Since readings in which ten well-defined waves could not be observed in succession were discarded, and since only the larger wave trains were the best defined, it is believed that this procedure gave an estimate of the wave period which is of the same order of magnitude as the significant wave period.

3-6 Drogues

To estimate currents at various depths, drogues (figure 3-6) were used. Each drogue consisted of a piece of plywood 24" x 24" x 1/2" to which a metal vane was attached by a length of 1/8" nylon cord. The vane was made of 24 gage galvanized iron and consisted of four mutually perpendicular arms, each arm being 12" x 12". The length of cord was adjusted so that the vane was supported at the desired depth by the plywood float which also served as the surface marker for the position of the vane.

Ideally, the vane should travel at the velocity of the current averaged over the 12" vane height at the depth determined by the length of the supporting cord. The speed of the drogue is affected

by the fact that the float and the cord are in zones of current velocity different from that at the vane. Thus the speed of the drogue is not exactly equal to the current velocity at the vane depth. In addition, the velocity differential may cause the supporting cord to hang at some angle to the vertical so that the vane is at some depth less than the length of the supporting cord. This means that the drogue velocity is representative of the current at some depth less than that reported. The two effects operate in an additive manner to make the reported velocity greater than the true velocity at the reported depth.

In this general study, this error was not considered to be too significant for qualitative use, and the drogue velocity was recorded as the velocity of the current at the depth equal to the length of the supporting cord.

Drogue velocity was estimated by measuring the time of travel between two buoys. Normally, the buoys were spaced two hundred feet apart for these tests.

3-7 Equipment Calibration

A laboratory investigation was conducted to calibrate the instruments and to determine the characteristics of the fluorescence phenomena of Rhodamine B in the aquatic environment of the experiment.

Since temperature is the most significant enviromental influence on the fluorescence of Rhodamine B, it was necessary to obtain

correction factors to convert the fluorescence at the sample temperature to that at a standard temperature. A fifteen liter sample of lake water was cooled to 7°C, and Rhodamine B was added to provide a known concentration. The sample was pumped through the fluorometer-thermometer system used in the field. The system was operated continuously in a closed circuit by discharging the water into the original container. As the temperature of the sample increased, the temperature and fluorescence were recorded. Taking 25°C as the standard temperature, the correction factor (fluorescence at 25°C divided by fluorescence at temperature, θ was plotted against sample temperature, θ as shown in figure 3-7.

By a similar procedure, the equipment was calibrated for concentration of Rhodamine B in terms of its fluorescence. Using the continuous flow system in a closed circuit, the temperature and fluorescence were recorded as the dye concentration was increased. By means of the previously prepared temperature correction curve, the fluorescence values were corrected to the 25°C standard. This standardized fluorescence was plotted against the concentration of Rhodamine B in figure 3-8. The fluorescence was found to be nonlinear with concentration. This agrees with the report of Feuerstein and Selleck.

The following equations express the c-F relationships on the four sensitivity ranges of the fluorometer used.

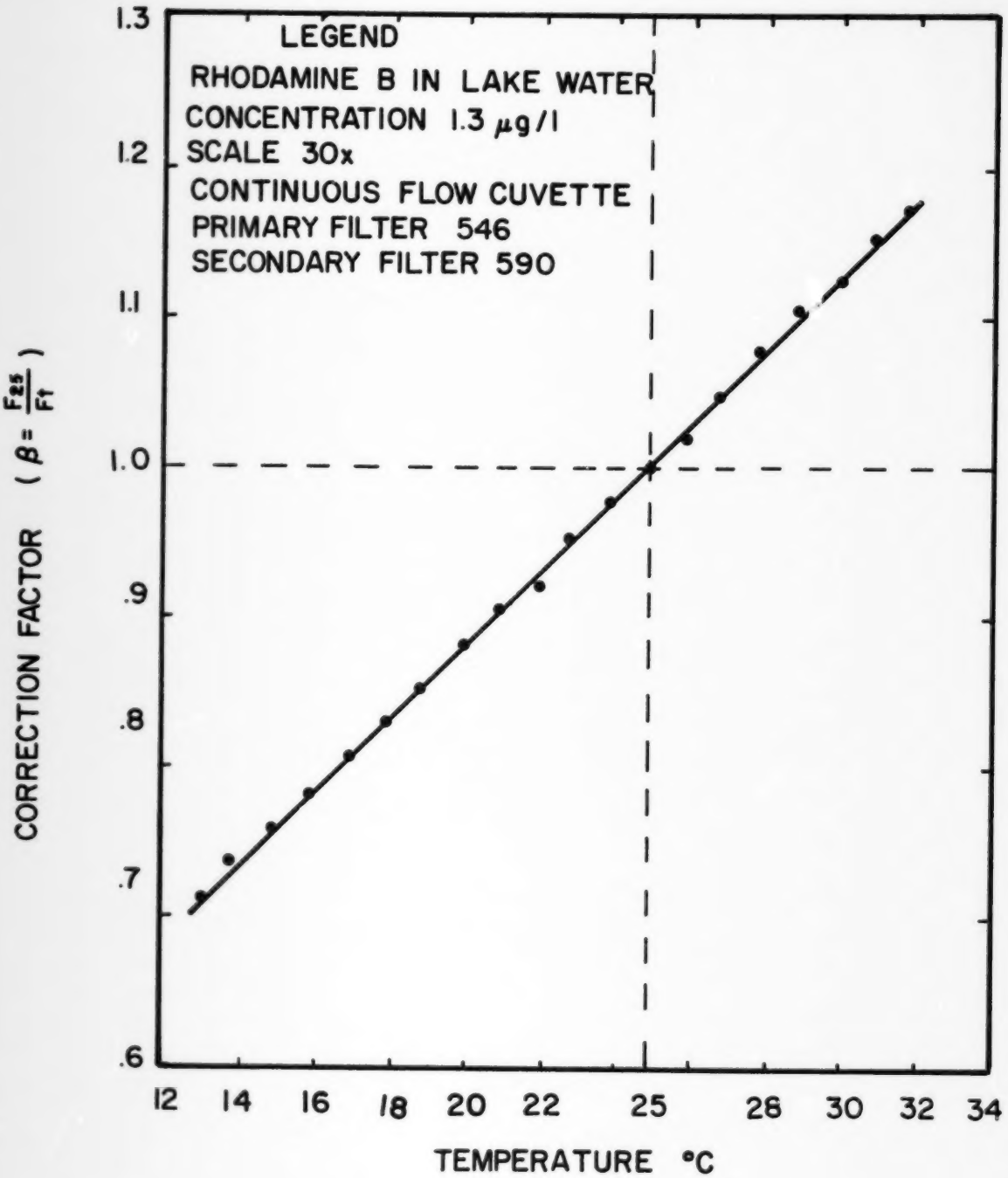

Fig. 3-7 Temperature Correction

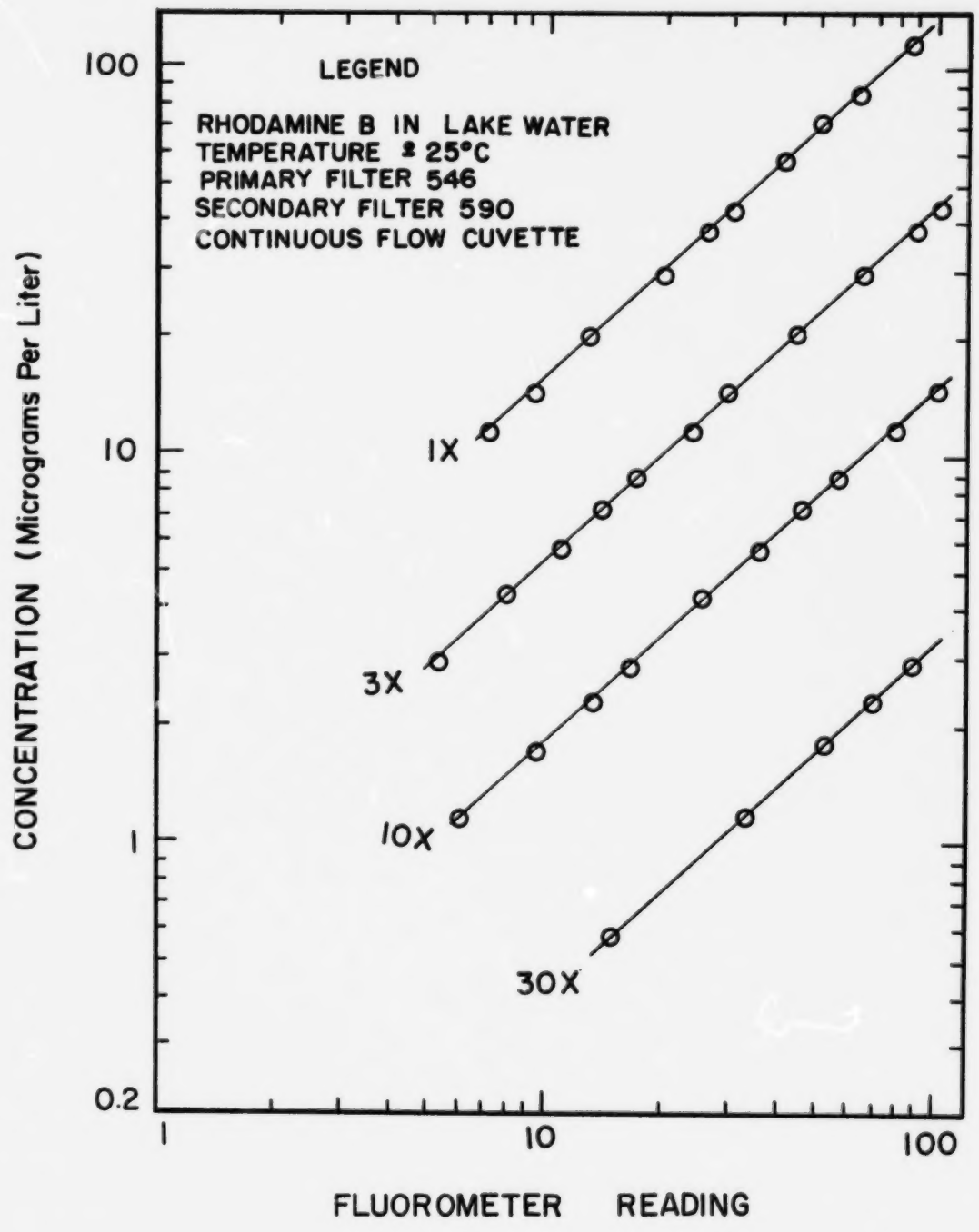

Fig. 3-8 Calibration Curves For Concentration vs. Fluorescence

$$1x : \quad c = 2.0\,(F_{25})^{0.9} \qquad (3\text{-}3a)$$

$$3x : \quad c = 0.67\,(F_{25})^{0.9} \qquad (3\text{-}3b)$$

$$10x : \quad c = 0.225\,(F_{25})^{0.9} \qquad (3\text{-}3c)$$

$$30x : \quad c = 0.0503\,(F_{25})^{0.9} \qquad (3\text{-}3d)$$

where c = concentration of Rhodamine B in micrograms per liter and

F_{25} = fluorescence reading at 25°C.

The discrete sample cuvette was calibrated in a similar manner.

3-8 Experimental Methods

To measure the dispersion of dye from an instantaneous point source, a measured quantity (50 to 250 ml) of 40% Rhodamine B in acetic acid solution was mixed with 1 or 2 gallons of water taken from the lake immediately before the test. The mixture had very nearly the same density as the receiving water so that dispersion was unaffected by the density difference.

The dye mixture was carefully introduced at the surface of the lake with as little mechanical mixing as possible. The dye was poured very slowly from a container onto a piece of plywood floating on the water surface. This procedure seemed to give a minimum of initial dispersion, especially in the vertical direction.

After the dye had dispersed for measured periods of time, the boat was driven across the apparent center of the cloud at a constant velocity while the water was continuously sampled and the fluorescence recorded along with the temperature. The velocity of the boat was determined by timing the travel over a measured 200' distance. The distance was determined by dragging a floating marker 200' behind the boat with a floating ski rope past a buoy while traveling in the same direction as when sampling.

A one gallon plastic bottle (bleach or detergent container) with the bottom removed will float submerged with the upper surface almost exactly level with the water surface. These containers were found to be useful as reference points for the moving cloud of dye. The containers floated with very nearly the same velocity as the cloud and, if relocated after each pass, would serve to mark the position near the center of the cloud where the previous reading was made. With the "float-dragging" method of measuring boat velocity, the velocity of the boat relative to the cloud could be estimated by using the marker bottle as a reference rather than an anchored buoy.

Both longitudinal and lateral profiles of concentration were made by continuous sampling, and periodically, vertical profiles of discrete samples were collected for later fluorescence measurement.

In tests of the dilution rate, it was possible to reduce the

amount of mechanical mixing from the boat and motor. To do this, the boat was paddled or allowed to drift to the apparent center of the cloud. Here, the pump was started and the boat maneuvered with a paddle to find the point of maximum concentration. Time, fluorescence and temperature were continuously recorded and a group of discrete samples for a vertical profile were collected periodically at the point of maximum concentration. The dilution rate seemed to be unaffected by the boat and motor when these results were compared with those of tests made by using the motor to maneuver the boat through the cloud of dye.

Surface current speeds were measured by averaging the time of travel of six plywood floats 8" x 8" x 1/4" between two buoys anchored a known distance apart--usually two hundred feet. Current velocities were measured before, after and, as time permitted, during each test. The velocity of a surface float varies greatly with the height of the surface exposed to the wind and with the depth of the float. The painted 1/4" plywood pieces floated with very little free-board exposed to the wind and were more durable and more easily located than pieces of paper which would more closely represent the movement of the surface film.

3-9 Test Sites

The test sites are located in Lake Travis, largest of the Highland Lakes of central Texas. Impounded by Mansfield Dam which was con-

structed by the United States Bureau of Reclamation in 1934, Lake Travis serves for flood control, irrigation and power generation. The Lake is 65 miles long with 270 miles of shore line and a maximum depth of 225 feet. The surface is 42,000 acres, and the capacity is 2 million acre feet.

The experiments were conducted at three sites. (see figure 3-9). Site 1 is located near the center of the Lake between Windy Point and the dam. Here the Lake is approximately two miles wide with a depth greater than 200 feet. Site 2 is located farther up the lake between Arrowhead Point and Starnes Island. At this location the lake is approximately three-fourths of a mile wide, more than 180 feet deep, and winds from the southeast have a fetch of approximately three miles. Site 3 is located in Long Hollow, a long, narrow canyon north of Starnes Island. Here the lake is approximately 150 feet wide and well protected by hills. Only the tests of dilution rate were made at site 3.

During the period of the tests, the thermocline was located at a depth of approximately 35 feet. Measurements of dissolved oxygen showed the upper layers to be well mixed.

Reproduced from
best available copy.

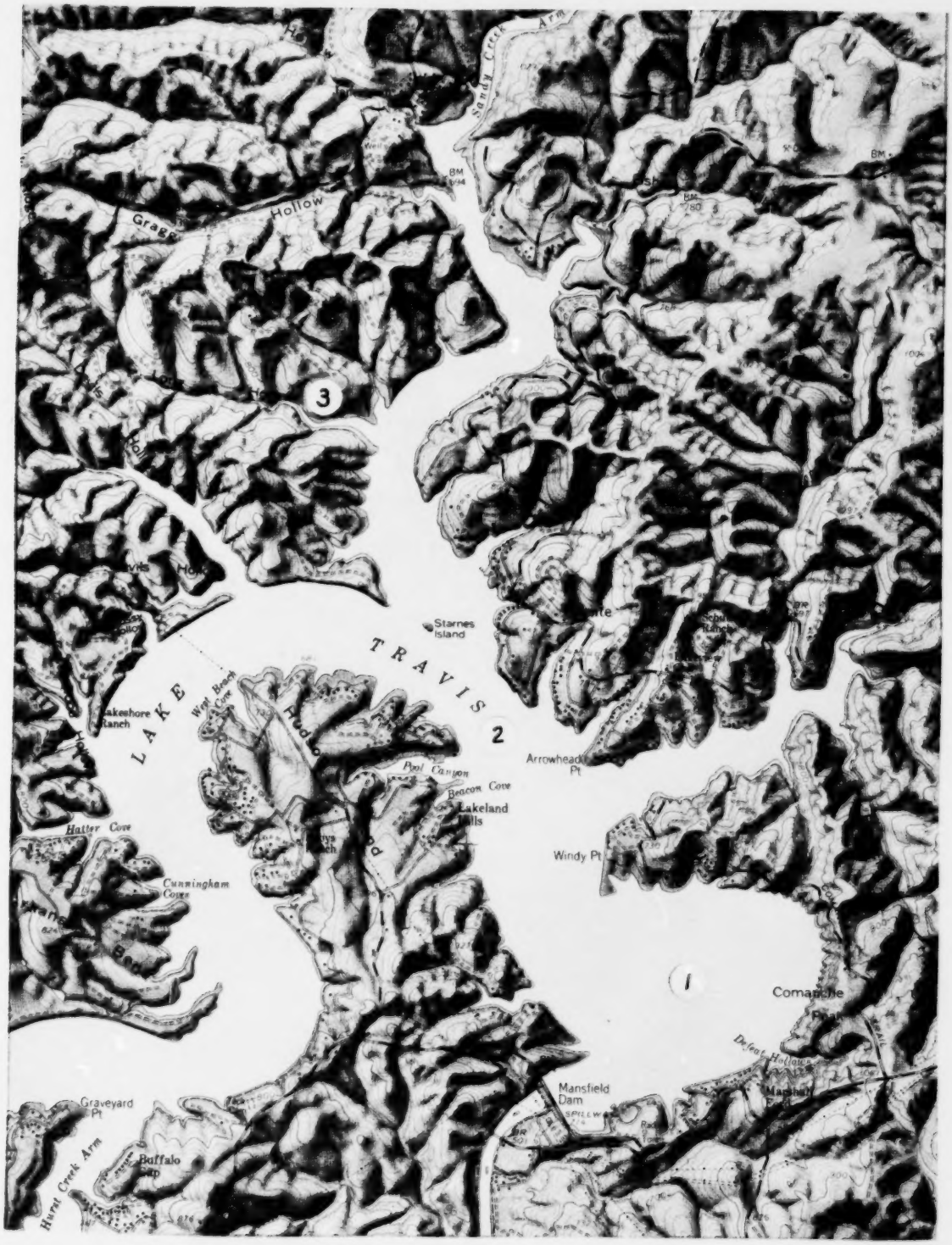

Figure 3-9 MAP OF TEST SITES (Scale 1:62500)

CHAPTER 4

EXPERIMENTAL OBSERVATIONS AND RESULTS

4-1 General

As noted previously, the general purpose of the experimental research presented herein was to investigate the mixing and dispersion processes in a deep lake or reservoir. The first phase of the investigational program was, therefore, devoted to general qualitative investigations to gain some understanding of the phenomea existing in the lake selected as the site for the study.

Estimates were made of the currents at various depths. Observations were made of the dispersion of groups of floating objects as well as the dispersion of dye clouds from the instantaneous releases and of dye plumes from continuous releases.

It became obvious immediately that the behavior of the dispersant depended very strongly on the variability of the wind and the wind-driven currents. Changes in wind velocity and direction cause very complex current patterns. For example, when the wind changes direction, there is some lag before the surface current is changed to correspond to the new wind direction, and there is considerably more lag before the effect is evidenced in the deeper layers of water. It was not uncommon to find the current at ten feet below the surface to be ten or fifteen degrees to the right of the surface current while that at the thirty-five foot depth was at some angle to the left.

Changes in direction of transport change the orientation of the coordinate axes (which are normally defined in relation to the direction of transport) with respect to the cloud, and no meaningful data could be collected for the horizontal dispersion coefficient when the wind direction was variable. Measurements of the horizontal dispersion coefficient were, therefore, limited to those days when fairly well-established, regular currents were found.

4-2 Difficulties Encountered

At this point it seems desirable to point out some of the difficulties encountered in making these tests from a small boat in a large, deep lake. Much of the scatter in the correlations to be presented later can be attributed to the inaccuracies caused by these problems:

(a) Location of reference points.

One of the reasons for the inability to collect meaningful data during conditions of changing wind directions was the lack of fixed reference points in the lake. For the continuous source test, one must be able to make traverses through the plume at right angles to the direction of transport. It is also desirable that several traverses be made at the same distance from the source. If the plume changes location because of change in wind direction, the marker range of buoys must be relocated. The mechanics of this operation, however, is overwhelming.

Since the buoys are anchored by long ropes in very deep water, a change in the current direction will change the buoy location. As a result of the elasticity of nylon line a 3° inclination of the buoy rope from the vertical would be a very conservative expectation, but in 180 feet of water, this permits the buoy to move about in a circle of 19 ft. diameter ($2 \times 180 \times \text{Sin } 3^{\circ} = 19$). For this reason the distance between buoys or between buoys and lines through shore ranges must be checked frequently as the current varies.

(b) Currents.

The combination of currents, winds and deep water make holding the boat in a fixed position with respect to the earth or to the dye cloud impractical. Anchoring in this depth is of no help and mooring to two or more anchors is impractical.

Steering a line normal to the direction of the wind and current and straight with respect to the moving cloud of dye requires imagination as well as considerable skill and judgment. The component of the boat's velocity in the down-wind direction is always much greater than the velocity of the cloud in that direction.

(c) Waves

The wave action very seriously affects the sampling depth. The pitching or rolling of the boat and the uneven water surface combine to move the pump intake through a wide range of depths. The intake must be kept well below the surface to avoid air bubbles which affect the fluorescence reading.

The rolling and pitching also affect the ability of the crew to perform their duties. In an 8" wave condition, for example, the act of setting a buoy with the minimum amount of line from anchor to surface becomes a chore.

(d) Boat velocity measurements.

Current meters can be used to measure the velocity of the boat with respect to the water at the depth of the meter. If the boat velocity with respect to the earth is desired, the best method is to time the travel over a known distance. For measurement of velocity of the boat with respect to the cloud of dye, the method is to time the travel between reference points located a known distance apart and moving at the speed of the cloud.

For the velocity relative to the earth, a float was towed 200 feet behind the boat. The time was measured from the instant at which the boat stern cleared a buoy until the float cleared the same buoy. For velocity relative to the cloud, the float was towed past a floating marker which was adjusted to travel at the same velocity as the cloud.

These velocity measurements are quite time-consuming, and they are not as accurate as one would desire.

4-3 Continuous Flow Source vs. Instantaneous Release

To measure the dispersion coefficients, two types of tests were made. The tests differed in the method of dye release. In one type, the

dye was released in a slug or instantaneous point source. The dye cloud was followed and, at time intervals, concentration profiles were measured in the three coordinate directions: x, y, and z. The dispersion coefficients were calculated for each profile by: $D = \frac{1}{2} \frac{d(\sigma^2)}{dt}$ or plotting σ vs. $\sqrt{t}$ and measuring the slope of the line of best fit. The slope is equal to $\sqrt{2D}$.

In the other type of test, the dye was released in a continuous flow from the fixed point. The source was a constant head tank similar to that described by Csanady (1963). The spreading plume gave a colorful illustration of the dispersion, but the quantitative results obtained for the dispersion coefficients are questionable. In the first place, the longitudinal dispersion coefficient cannot be calculated from the continuous flow test. The lateral and vertical coefficients may be calculated from "instantaneous" profiles of concentration taken in the plume at a known distance, x, from the source as

$$D = \frac{1}{2} \bar{u} \frac{d(\sigma^2)}{dx} \qquad (4\text{-}1)$$

The uncertainty concerns the measurement of $\bar{u}$, the mean velocity of the plume. In his calculations, Csanady used the velocity of the visible leading edge of the dye plume, a method which requires the following assumptions:

(1) It assumes that the velocity of the leading edge is repre-

sentative. This is not true unless there is no longitudinal dispersion. One may observe that in a diffusing cloud the leading edge moves much faster than the mass center. If this were not true, there would be no longitudinal dispersion.

(2) It assumes that the visible leading edge velocity is the same as the velocity at the depth of the sampling intake. In a wind driven current near the surface, the velocity decreases very rapidly with depth. Depending on the dye visibility in the water and on the sampling depth, this assumption may be true or it may err by an order of magnitude.

(3) It assumes that the velocity which could be measured only one time (at the start of the flow) is constant and does not vary during the entire test.

Since the above assumptions were not valid in the study reported herein, no data from continuous flow tests were used to estimate the magnitude of dispersion coefficients.

In measuring the effect of scale on the diffusivity, however, the continuous flow source is much preferred over the instantaneous release. In this calculation, we are most concerned with correlating the relative change in the diffusivity with the dimensions of the plume. If the velocity of the current can be assumed to remain

constant during the series of tests, the effect of the current velocity is eliminated by studying the relative change in diffusivity.

Use of the continuous source in measuring relative changes in the dispersion coefficient is advantageous for several reasons:

(1) Many measurements can be made at a chosen distance and the resulting concentration profiles averaged. This reduces statistical error and gives much more confidence to the resulting value of relative diffusivity. Since measurements in a cloud dispersing from an instantaneous source are made at points in time, no measurement can be repeated for averaging purposes.

(2) The interval can be taken as small as is desired in order that the value of $\frac{\Delta \sigma^2}{\Delta x}$ will more nearly approach the derivative $\frac{d(\sigma^2)}{dt}$ at the point. With the instantaneous source, the measurements take a certain amount of time, and another interval of time must pass before the boat can be brought into position to make a second measurement.

4-4 Velocity Distribution

When wind blows over the surface of a body of water, it causes a shear stress at the air-water interface and drags the water along. Because of the viscosity of the water (and this includes eddy visocity), momentum is transferred to adjacent deeper layers of water and the

current penetrates more deeply. The velocity distribution in the vertical direction is obviously dependent upon the constancy of the wind. In one typical test, Haines and Bryson (1961) found that the surface current responded almost immediately to the wind shift, but the current at 20 to 30 centimeters below the surface lagged by 20 minutes while that at the 2 meter depth lagged by 90 minutes.

Since information concerning the vertical velocity distribution in an equilibrium condition was desired during the preliminary investigation, estimates of the currents existing at various depths were made by using the drogues described in Section 3-6. The drogues do not measure the current velocity with the accuracy desired, but the results are sufficiently accurate for a qualitative study to provide general information about the phenomena existing in the lake.

The velocity distribution is very important in the mixing process. The dispersion is greatly accelerated by the shear flow from velocity differentials existing between the layers of the water. Material which diffuses from a zone of high velocity into one of low velocity is later diffused back into the zone of high velocity. The direction of diffusion is in the direction of the concentration gradient and, as the higher velocity current transports its material forward leaving little or none adjacent to the material in the lower velocity zone, the gradient of concentration is reversed.

Taylor, as was noted in Chapter 2, found the longitudinal

diffusivity to be far greater than the lateral diffusivity in a pipe. The difference was a result of the velocity differential which existed laterally across the pipe. Elder developed a similar relationship for channel flow.

The velocity distribution in a wind-driven lake current is quite different from that in a pipe or in an open channel. The water is dragged along the shear stress from the wind rather than being caused by an energy gradient. In addition, there usually exists at some depth near the bottom of the lake a counter current which is necessary to maintain continuity.

Figure 4-1 shows plots of normalized velocity distribution with depth for surface conditions with and without whitecaps. The line of $[1 - u/U_s] \sim d^{1/7}$ is shown for comparison with Blasius smooth pipe relationship where $u/U_{max} \approx (y/r_o)^{1/7}$. There is considerable scatter which is most likely caused as much by a lack of true equilibrium conditions as by the inaccuracies inherent in the current velocity-measuring devices used, but the $d^{1/7}$ relation seems to fit the data reasonably well.

The tests were not made at the same location in the lake, nor were they made with the same conditions of stratification. Some tests were made in March before the thermocline had formed, and others were made in June and July after the lake was well-stratified with a thermocline existing at a depth of 35 to 40 feet below the surface.

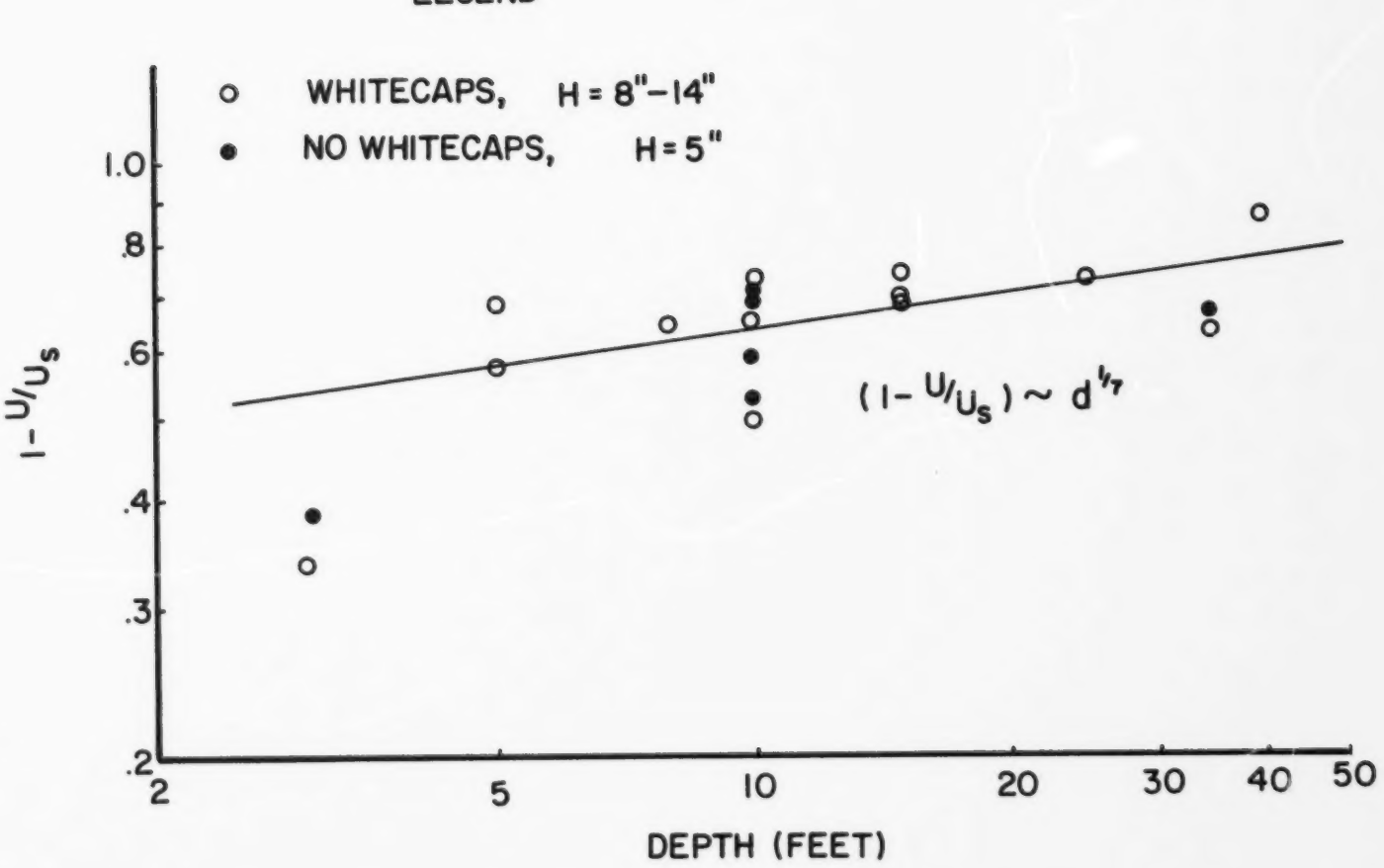

Fig. 4-1 Velocity Distribution With Depth

Table 4-1 lists the results of two sets of measurements made at the same location in the lake on the same date. The currents were flowing in the same direction, but because of a change in wind velocity, the surface condition and current velocities were quite different. Compared with the morning conditions, the afternoon measurements show greater velocities at all depths, larger wave heights, and a white cap condition which indicates greater turbulence--at least the turbulence is greater near the water surface. When the velocities are normalized by dividing each velocity by the surface velocity, the two conditions have vertical velocity distributions which are very similar. Thus the distribution of velocity appears to be independent of the surface conditions as well as of the magnitude of the velocity.

TABLE 4-1

	Morning Test 5 inch wave No whitecaps		Afternoon Test 8 inch wave Many whitecaps	
Depth (Feet)	Velocity(FPS)	U/U_s	Velocity(FPS)	U/U_s
0	0.37	1.00	0.72	1.00
10	0.17	0.46	0.36	0.50
35	0.13	0.35	0.27	0.37

4-5 Dilution Rate

One of the questions confronting the sanitary engineer in the study of mixing processes concerns the dilution rate, i. e., the rate

of diminution of the peak concentration in a dispersing cloud. In Section 2-1, there were presented several theoretical models for the prediction of the relationship between peak concentration and time of spread in a two dimensional system.

(a) The equations of Joseph and Sendner, of Okubo and Pritchard and of Schonfield all give a decrease in peak concentration which is inversely proportional to the square of time.

(b) Ozmidov, Okubo and Obhukov all show the peak concentration decreasing inversely as the cube of time.

(c) The Fickian solution gives a 1/t relationship.

Using the Fickian solution for a three dimensional system, Diachishin (1963) theorized that the peak concentration initially decreased as the minus three-halves power of time. After the cloud had reached the bottom and become uniformly distributed in the vertical direction, he considered the system to be two dimensional and the peak concentration decrease to be inversely proportional to time.

Okubo (1962), noting that the data available to him were accompanied by some uncertainty and that they offered little evidence of the true relationship, gave three plots of percent concentration vs. time. All relationships were in the vicinity of t^{-2} to t^{-3}, but there were few points and considerable scatter in each.

Pritchard and Carpenter (1960), from data collected in two experiments in Chesapeake Bay, showed two plots of the ratio of peak concentration to the weight of dye discharged times the vertical thickness of the layer containing the dye vs. time. One plot of three points observed over a period of 52 hours fit a $t^{-2.5}$ relationship. The other plot of 11 points observed over a period of 180 hours fit the t^{-2} relationship reasonably well.

In order to investigate the behavior of the peak concentration with time in this experimental research, the maximum concentration in a dispersing cloud of Rhodamine B dye was determined at various points in time by fluorescence measurements made in the manner described in Section 3-8. As the boat was maneuvered through the dispersing cloud of dye, fluorescence, temperature and time were continuously recorded on a strip chart.

The fluorescence values were converted to dye concentration by means of the calibration charts. The values of peak concentration (c) were made dimensionless by dividing them by the initial concentration of the dye mixture introduced (c_o).

Figure 4-2 shows the relationship between the relative concentration (c/c_o) and time for nine tests. In the first eight tests, P - 1 through P - 8, the dye was mixed with a small quantity of lake water (1 or 2 gallons) so that the mixture introduced had very near-

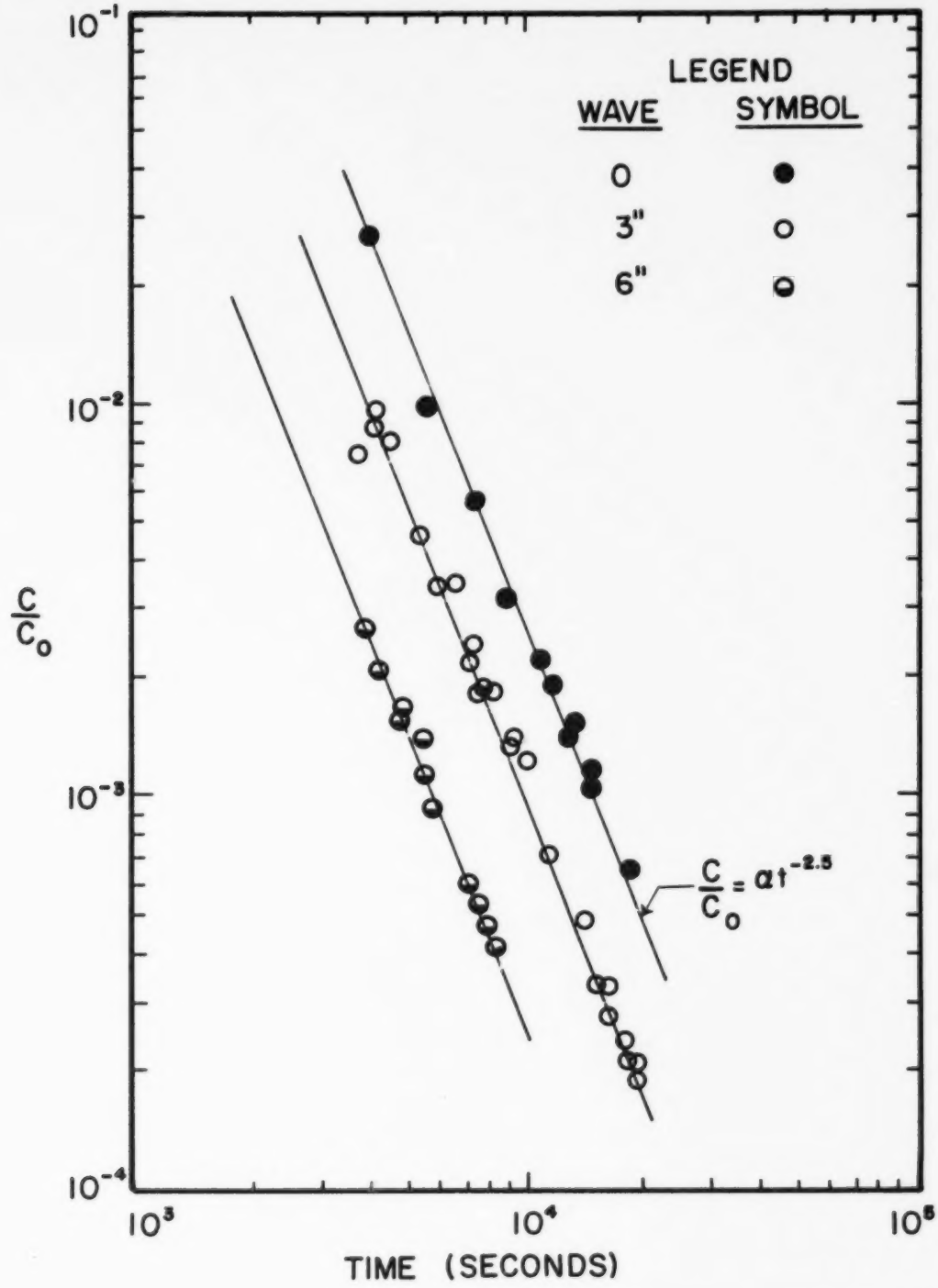

Fig. 4-2 Decrease in Relative Concentration With Time

ly the same density as the receiving water. This was done to reduce the effect of a density difference on the dispersion. In test P - 9, however, the dye was mixed in one gallon of methanol to provide a cloud of specific gravity less than the receiving water. This was done to restrict the dispersion to two dimensions.

The dilution rate tests were not limited to conditions of well-established currents nor of any equilibrium. Tests were made in three locations in the lake with very different characteristics. In test P - 8, for example, the wind reversed direction completely and later veered through 90^{o} to transport the cloud into the bank. During the sampling period, the cloud grew to approximately 1500 feet in length along the bank while the width was approximately 15 feet. The bank was a near-vertical wall very irregular in plan view. Even in this complicated boundary situation, the peak concentration is seen to fit the $t^{-2.5}$ relationship.

Table 4-2 shows the slope of the least squares line of fit for each set of data as calculated from:

$$\text{SLOPE} = \frac{\Sigma XY - {}^{1}/_{N}\,\Sigma X\,\Sigma Y}{\Sigma X^{2} - {}^{1}/_{N}\,(\Sigma X)^{2}} \qquad (4\text{-}2)$$

When X = log (time)

Y = log (relative concentration)

N = Number of data points.

Table 4-2 also shows the correlation coefficient for each set of data as calculated from:

$$\text{CORRELATION} = \frac{\Sigma XY - {}^1/_N \Sigma X \Sigma Y}{\sqrt{\Sigma X^2 - {}^1/_N (\Sigma X)^2}\sqrt{\Sigma Y^2 - {}^1/_N (\Sigma Y)^2}} \quad (4\text{-}3)$$

TABLE 4-2

Test	Slope	Correlation Coef.
P-1	-2.545	-0.996
P-2	-2.429	-0.994
P-3	-2.572	-0.998
P-4	-2.162	-0.998
P-5	-2.330	-0.995
P-6	-2.646	-0.999
P-7	-2.348	-0.999
P-8	-2.464	-0.999
P-9	-2.755	-0.997

The mean value of the slope is -2.47. Weighting on the basis of the number of data points in each test gives a value of -2.48 as the weighted mean.

This leads to a relationship in which the concentration decreases in proportion to the -5/2 power of time and agrees with none of the relationships proposed above.

Accordingly, the basic equation of Okubo (1962) was examined to determine the assumptions which must be made to obtain a result with the $t^{-5/2}$ relationship. The basic equation represents two dimensional diffusion in rotationally symmetrical space with generalized coefficient of diffusion, $k r^m f(t)$, and is:

$$\frac{\partial c}{\partial t} = \frac{1}{r} \frac{\partial}{\partial r}\left[k r^{m+1} f(t) \frac{\partial c}{\partial r}\right] \qquad (4\text{-}4)$$

where $\frac{\partial c}{\partial t}$ is the time rate of change of concentration, r is the distance from the center of mass, k is a constant, m is an exponent and t is the time after release.

The solution of the above equation under an initial condition that at $t = o$, $c(r, t) \rightarrow \frac{M}{\pi r} \delta(r)$ is given by:

$$C(r,t) = \frac{(2-m)\, M \exp\left[\frac{-r^{2-m}}{(2-m)^2 K \psi(t)}\right]}{2\pi (2-m)^{q/2-m} \Gamma\left(\frac{2}{2-m}\right) K^{\frac{2}{2-m}} [\psi(t)]^{\frac{2}{2-m}}} \qquad (4\text{-}5)$$

for $0 \leq m < 2$.

where M is the amount of substance per unit depth,

$\Gamma(a)$ denotes the Gamma function and

$$\psi(t) = \int_0^t f(t)dt$$

If it is assumed that the diffusivity:

(a) Is independent of time

$$[\, f(t) = 1 \,]$$

and

(b) Is proportional to the 6/5 power of the distance of the mass center

$$[\, m = 6/5 \,]$$

then the solution to the equation becomes:

$$C(r,t) = \frac{8M}{75\pi^{3/2}\omega^{5/2}t^{5/2}} e^{-\left[\frac{r^{4/5}}{\omega t}\right]} \qquad (4\text{-}6)$$

where ω is defined as a diffusivity parameter with dimensions of $[\text{feet}]^{4/5}$ per second.

The peak concentration is found at the mass center (r = o) and is:

$$C(0,t) = \frac{8M}{75\pi^{3/2}\omega^{5/2}} t^{-5/2} \qquad (4\text{-}7)$$

The diffusion coefficient is

$$D = \frac{25}{16}\omega r^{6/5} \qquad (4\text{-}8)$$

It may be shown that other assumptions can be made concerning the diffusivity to arrive at the $t^{-5/2}$ relationship. In fact

any combination such that:

$$f(t) = t^{\left(\frac{6-5m}{4}\right)} \qquad (4\text{-}9)$$

will provide such a solution. The assumptions made above, however, appear intuitively to be the most acceptable.

To assume the "4/3 law", that diffusivity varies with the 4/3 power of the scale, we must also assume that:

$$f(t) = t^{-1/6} \qquad (4\text{-}10)$$

in order to keep the $t^{-5/2}$ relationship in the result.

Test P-9, in which the dispersion was kept two dimensional by making the dye much less dense than the lake water, showed that the dilution rate was not decreased by restricting the dispersion to two dimensions. In fact, the dispersion rate was slightly higher in test P-9 than in any other test.

Since the concentration - time curve is a straight line and the slope is always $-5/2$, any point on the line will define it. Therefore, if the initial concentration at $t = 0$ is known, one measurement of the peak concentration at any later time will permit prediction of the peak concentration at any time in the future.

The diffusivity parameter, ω, depends upon the amount of turbulence present in the lake. ω determines the intercept of the concentration - time curve, and if it is known, future concentrations

can be predicted without making any measurements. Future study might well be directed toward finding easily-measured parameters which will predict the value of this diffusivity parameter.

In order to put the effect of all dilution phenomena into one coefficient in an empirical equation, equation 4-7 was modified to:

$$\frac{C}{C_0} = \alpha t^{-5/2} \qquad (4\text{-}11)$$

The dilution coefficient, α, which has the dimension of the $(\text{time})^{2.5}$, includes all of the terms in the fraction of equation 4-7 divided by the initial concentration of the cloud at time equal to zero.

Table 4-3 summarizes the results of the nine test runs. Figure 4-3 shows a plot of α vs. U_s. The least squares line of fit has a slope of -2.23 and the correlation coefficient is -0.97. Since breaking waves greatly increase the turbulence near the surface, a factor, K_c, is applied to the data to account for the different surface conditions. Figure 4-4 is a plot of α vs. $K_c U_s$, where K_c is defined as 1.00 for the "no-whitecap" condition and as 0.78 for the "whitecap" condition. The least squares line of fit has a slope of -3.05, and the correlation coefficient is -0.99. The relation is:

$$\alpha = K_c U_s^{-3} \qquad (4\text{-}12)$$

DATE	TEST	WAVE	U_s(fpm)	$\alpha \times 10^{-6}(sec^{2.5})$	SITE
5-30-66	P-1	6"	36	2.6	1
7-13-66	P-2	10"	32	2.8	1
7-19-66	P-3	3"	16	11.8	1
7-19-66	P-4	3"	17	10.5	1
7-20-66	P-5	3"	18	9.4	1
7-21-66	P-6	4"	19	6.4	2
7-22-66	P-7	Ripple	12	27.	3
7-25-66	P-8	Ripple	13	28.	3
8-18-66	P-9	Ripple	16	--	1

TABLE 4-3 DILUTION RATE TESTS

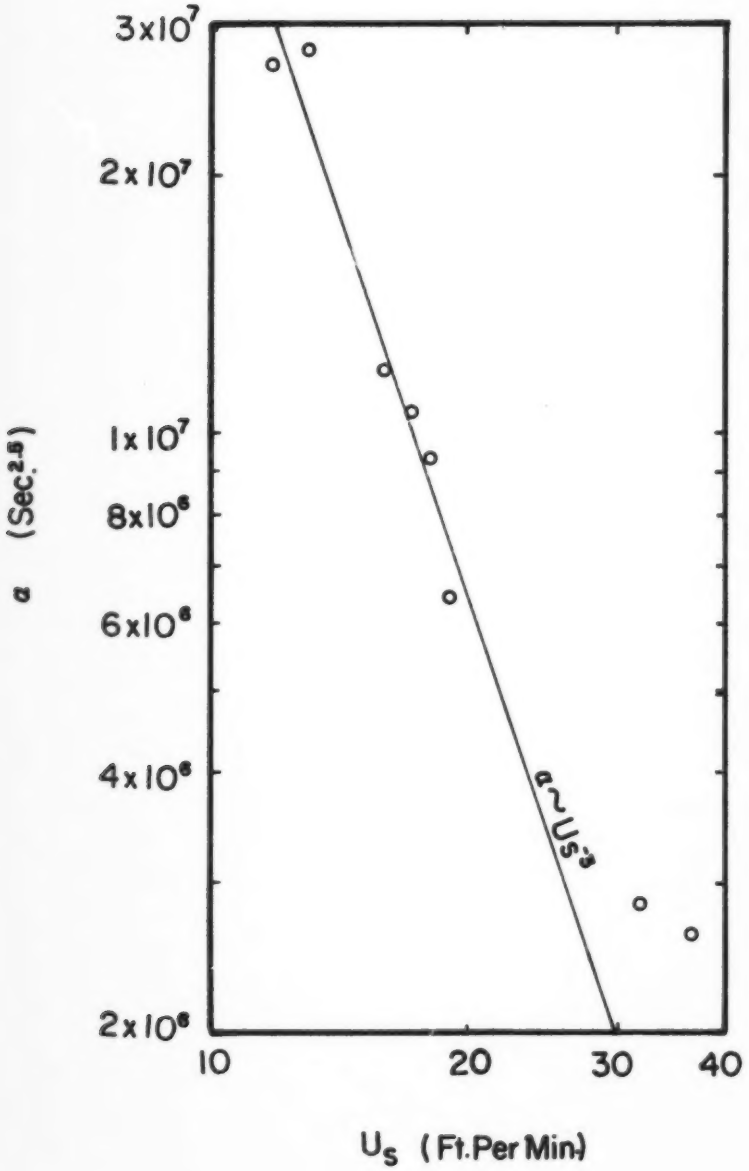

Fig. 4-3 Dilution Coefficient vs. Velocity of Surface Current

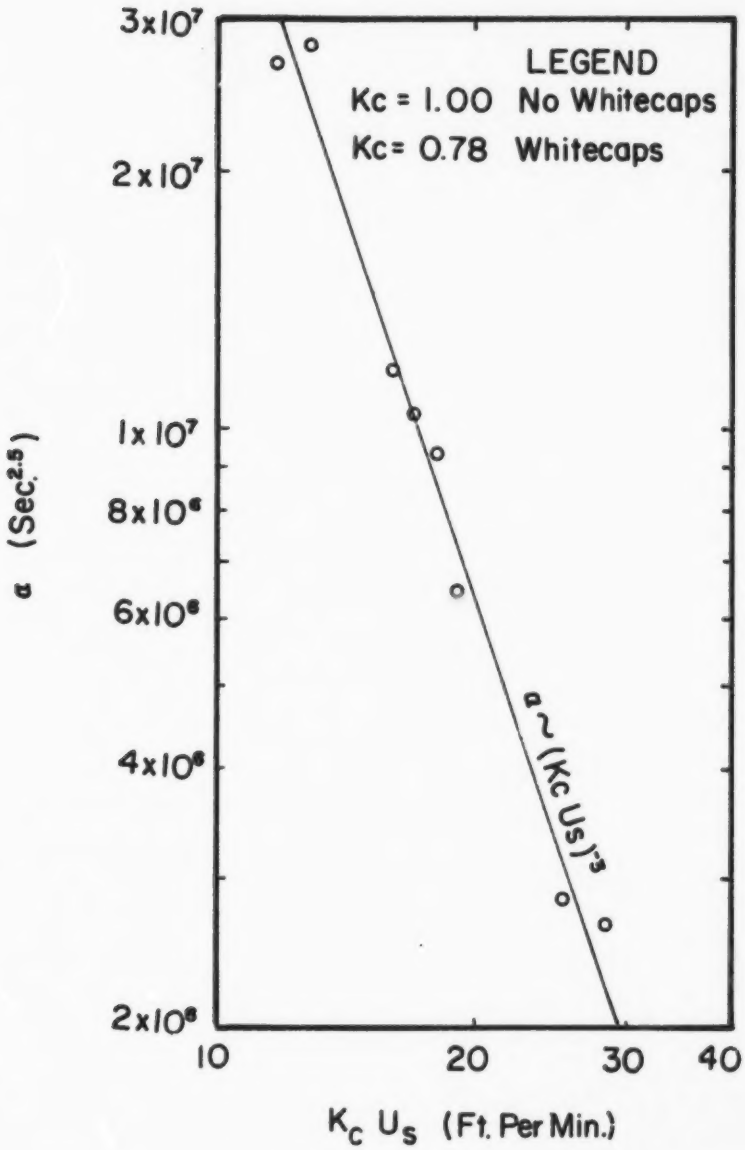

Fig. 4-4 Dilution Coefficient vs. Velocity of Surface Current Corrected for Surface Conditions

4-6 Vertical Dispersion

The coefficient of vertical dispersion was calculated from fluorescence measurements made with the vertical discrete sampling devices previously described. After the cloud of dye had dispersed for measured increments of time, sets of discrete vertical samples were collected and stored in polyethylene bottles until fluorescence measurements could be made with the discrete sample door mounted on the fluorometer. The time of storage was never more than four hours. Tests showed that there was no change in fluorescence of samples (when corrected for temperature change) stored for periods of twenty-four hours.

Figure 4-5 shows the vertical profile of dye concentration at various times for a typical test, test V-4 of June 29, 1966. As might be expected, the maximum concentration decreases and the dye becomes more uniformly mixed as time passes.

Since only the relative concentrations in each data set were needed for the calculation of the standard deviation, values of $F^{0.9}$ were used because:

$$c = k F^{0.9} \qquad (3\text{-}3)$$

Starting with the depth at which the minimum trace of dye was found, the accumulated values of concentration for each set of data were normalized to 50% and plotted on arithmetic probability paper at

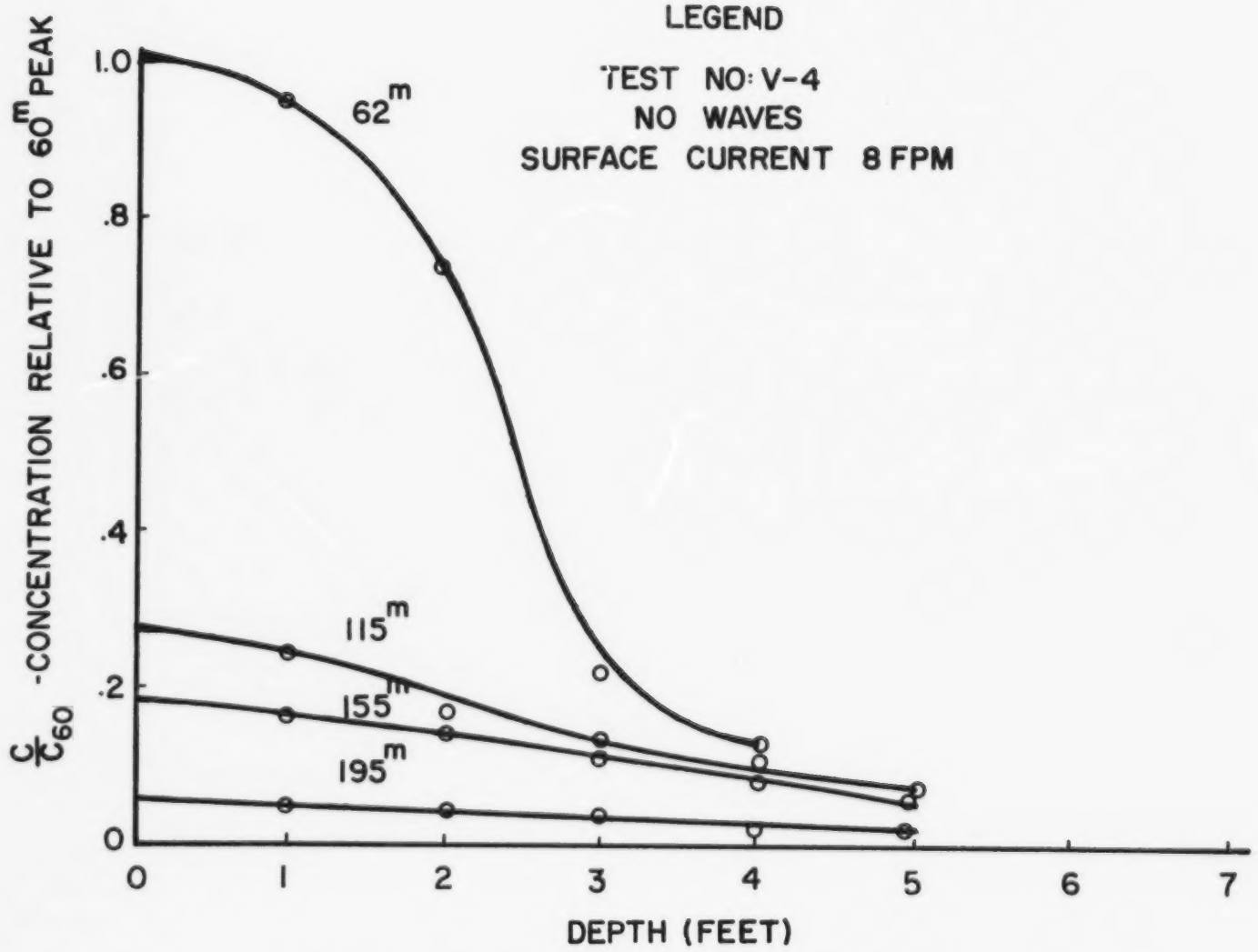

Fig. 4-5 -Vertical Concentration Profiles At Various Times

intervals corresponding to the spacing of the sampler bulbs. The resulting plots were well-fitted by a straight line indicating Gaussian distribution of the concentration. The standard deviation was estimated by the point at which the line intersected the line of 15.86% probability. In some tests, the data were incomplete and could not be accumulated in this manner. In these instances, the data were fitted with a Gaussian curve and the standard deviation measured. Figure 4-6 is an example of the data plotted on arithmetic probability paper.

The coefficient of vertical dispersion was estimated from the standard deviation by using equation (2-4). Results of the measurements are summarized in table 4-4.

Stewart and Grant (1962) found that energy dissipation varies with depth much less than does the wave energy. They noted that almost all wave dissipation is concentrated near the surface and is essentially all above the trough line. They suggest that the observed turbulence is more closely associated with the wind-driven drift current than with the waves.

Intuitively, it would seem that the surface current is a good parameter for describing turbulence in a system of wind-driven currents. The essentials of energy input into the wave system are wind velocity, duration and fetch. Because of the inertia of the water mass, the surface current represents the integral sum of the effect of the wind velocity over a period of time.

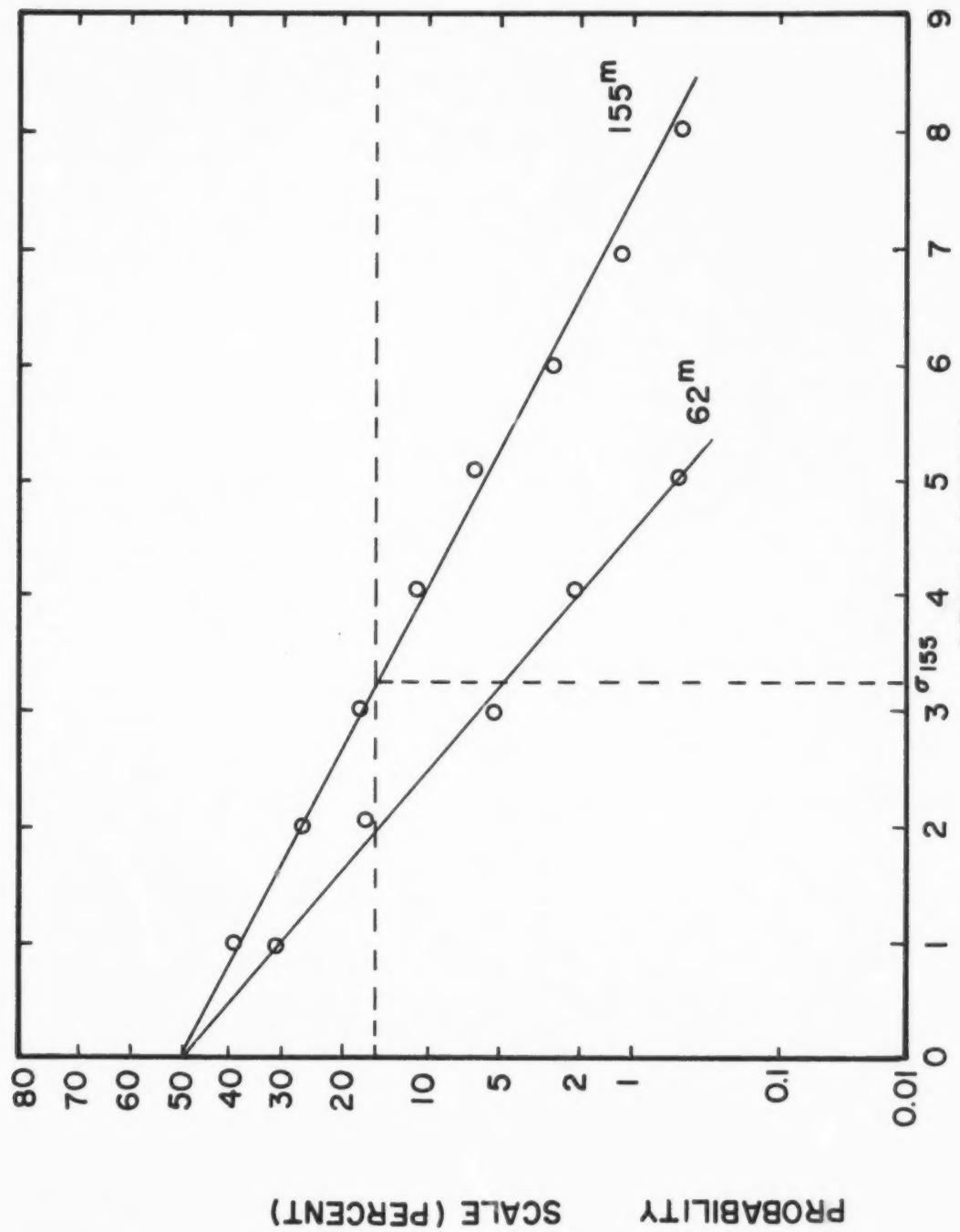

Fig. 4-6 Graphical Determination of Standard Deviation

TEST	H(in)	T(sec)	U_s(ft/sec)	D_z(ft^2/sec)
V1	0	-	0.18	0.00039
V2	6	1.2	.63	.00350
V3	5	1.0	.25	.00167
V4	Ripples		.11	.00057
V5	5	1.1	.43	.00102
V6	10	1.4	.53	.072
V7	3	0.9	.27	.00037
V8	3	0.9	.28	.00055
V9	3	0.9	.30	.00037
V10	4	1.0	.32	.00085
V11	Ripples		.20	.00034

TABLE 4-4 VERTICAL DISPERSION TESTS

Johnson (1959) reports that:

(1) Wind over water may cause mixing and dispersion of wastes by several different processes: surface currents by tangential shear stresses, turbulent wave action (when the wind speed exceeds 13.2 knots), mass transport by swell and surface slicks.

(2) The rate of increase of surface current becomes less as the wind speed increases and, since turbulence increases with the speed of the wind, rate of mixing increases above the straight line prediction.

Figure 4-7 shows a plot of D_z vs. U_s. The diffusivity generally increases with the surface current, but there is considerable scatter.

Figure 4-8 shows a plot of D_z vs. the velocity, $\frac{\pi H}{T}$, which is the approximate value of the maximum horizontal velocity of the water particles in deep water as they orbit in a vertical plane during the passage of a wave. There seems to be very good correlation, but there is very little variation in the calculated orbital speed throughout the series of tests, and the line is near vertical.

In figure 4-9, D_z is plotted against the velocity $U_s + \frac{\pi H}{T}$. The minimum value of D_z appears to be about 0.0004 sq. ft. per sec. When the value of $U_s + \frac{\pi H}{T}$ increases to approximately 1.5 ft. per sec., the value of D_z seems to be correlated better with the sum of the velocities than with either velocity separately.

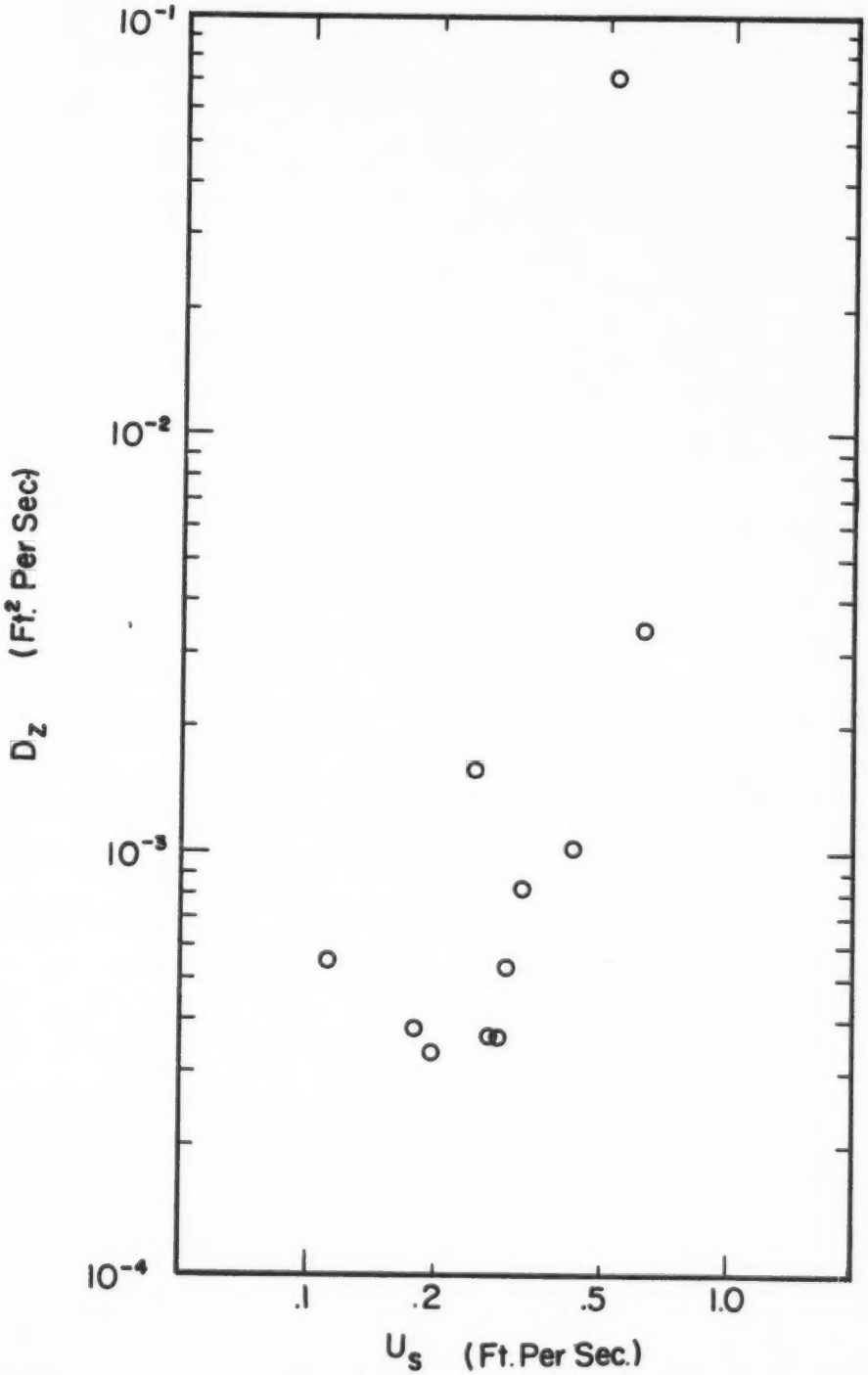

Fig. 4-7 Vertical Dispersion Coefficient vs. Surface Current Velocity

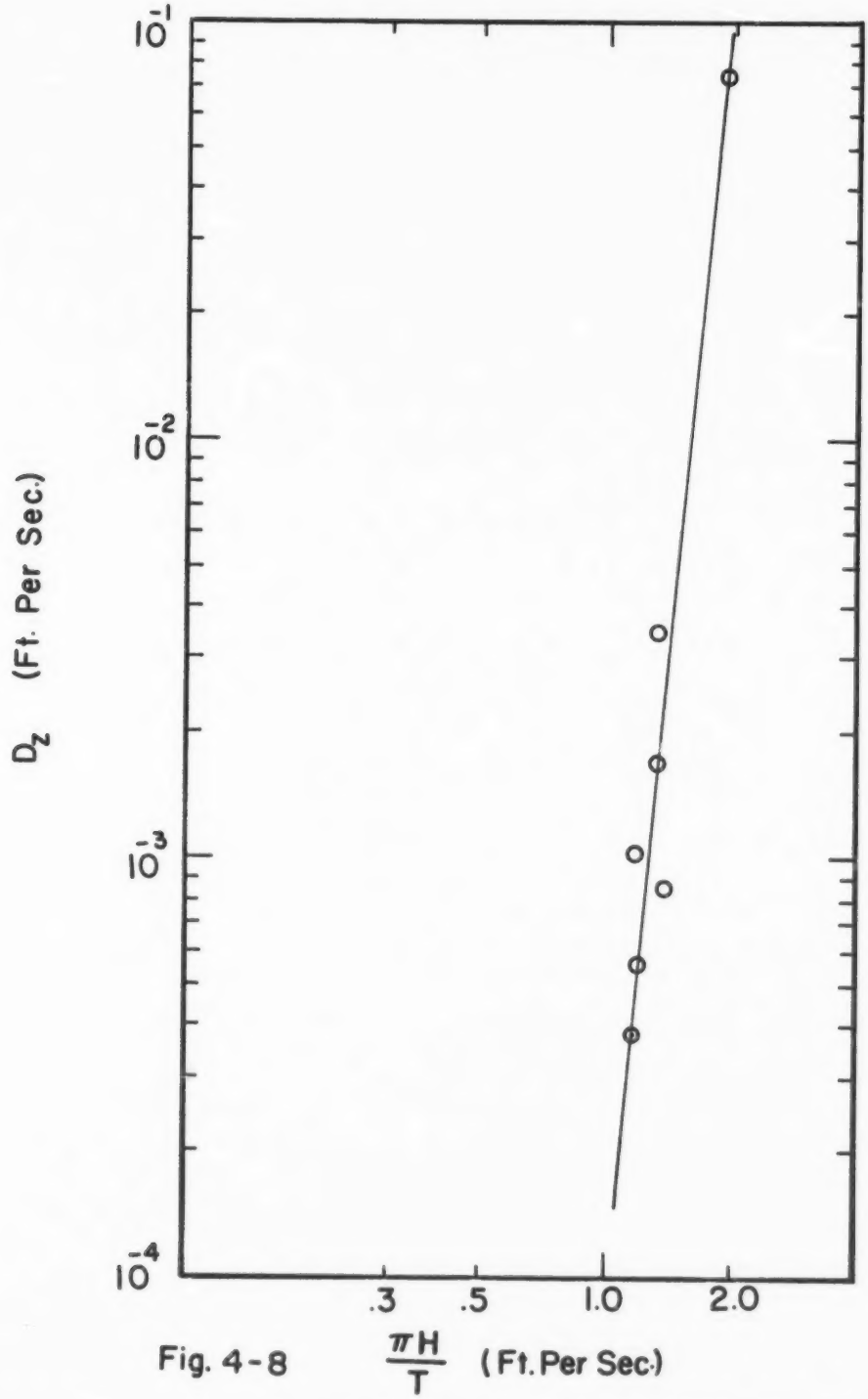

Fig. 4-8 Vertical Dispersion Coefficient vs. Water Particle Orbital Velocity

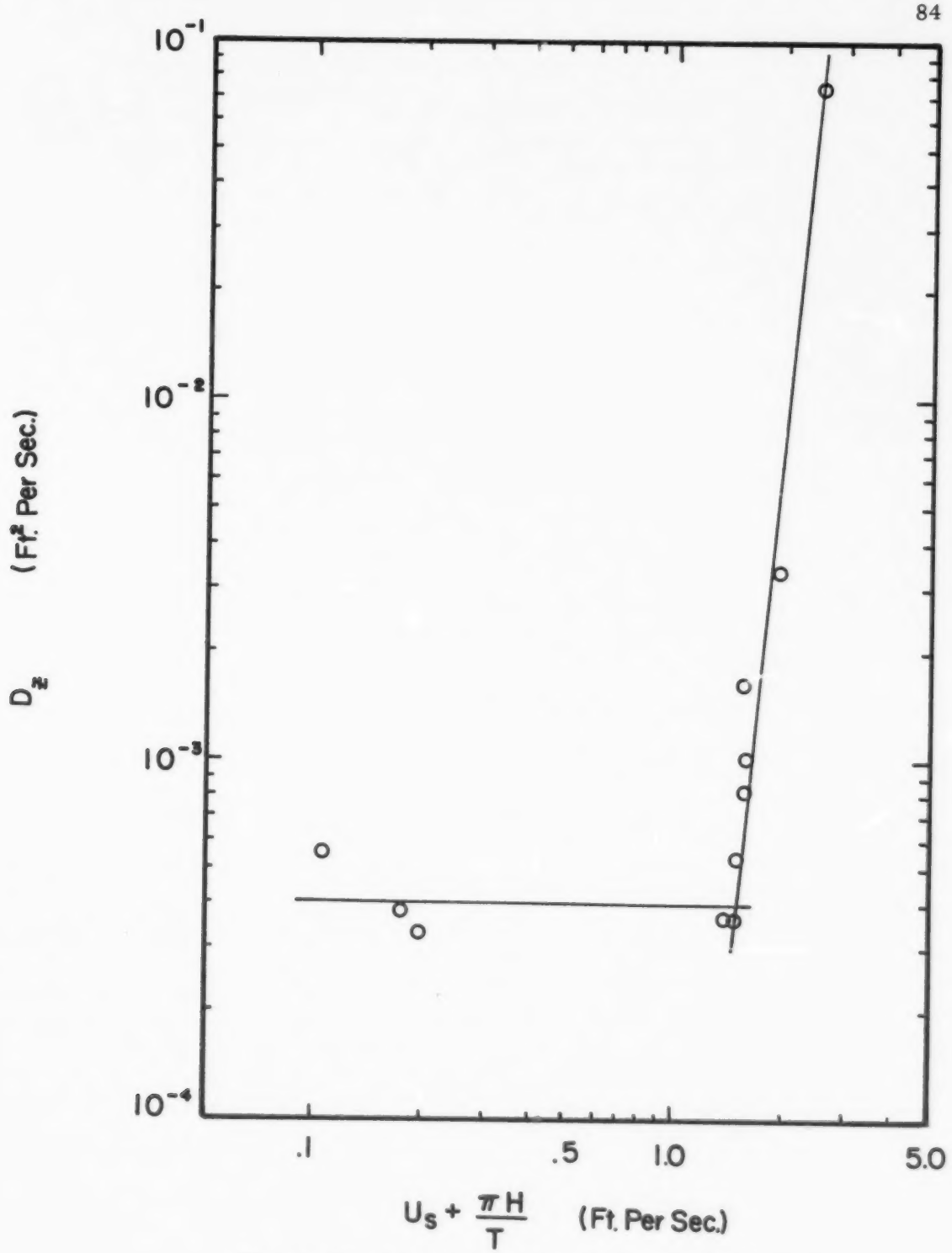

Fig. 4-9 Vertical Dispersion Coefficient vs. Total Velocity of Water Particle

Figure 4-10 shows D_z vs. H. At wave heights up to about 3", the value of the vertical diffusivity appears to be fairly constant at approximately 0.0004 sq. ft. per sec. At greater wave heights, $D_z \sim e^{H/3}$ appears to fit the data very well.

There is no change in the curve as a result of the breaking of the waves. This indicates that the vertical diffusivity is a function of the wave height but is independent of the whitecap condition.

4-7 Lateral Dispersion

The coefficient of lateral dispersion was calculated from fluorescence measurements made by the procedures described in Chapter 3 for the flow-through door. A known quantity of dye was introduced as a slug at the water surface and allowed to disperse. After measured increments of time, profiles of fluorescence were recorded on the moving strip chart as shown in figure 4-11. The pump intake was set as near to the surface as the wave conditions and boat movement permitted, usually a depth of 12" to 18". Since the speed of the boat and the chart speed are known, the chart abscissa may be converted to horizontal distance along the direction of boat travel.

A property of the Gaussian distribution is that at any given percentage of the peak value, the "bell" width is a fixed percentage of the standard deviation. For example, at approximately 88.8% of

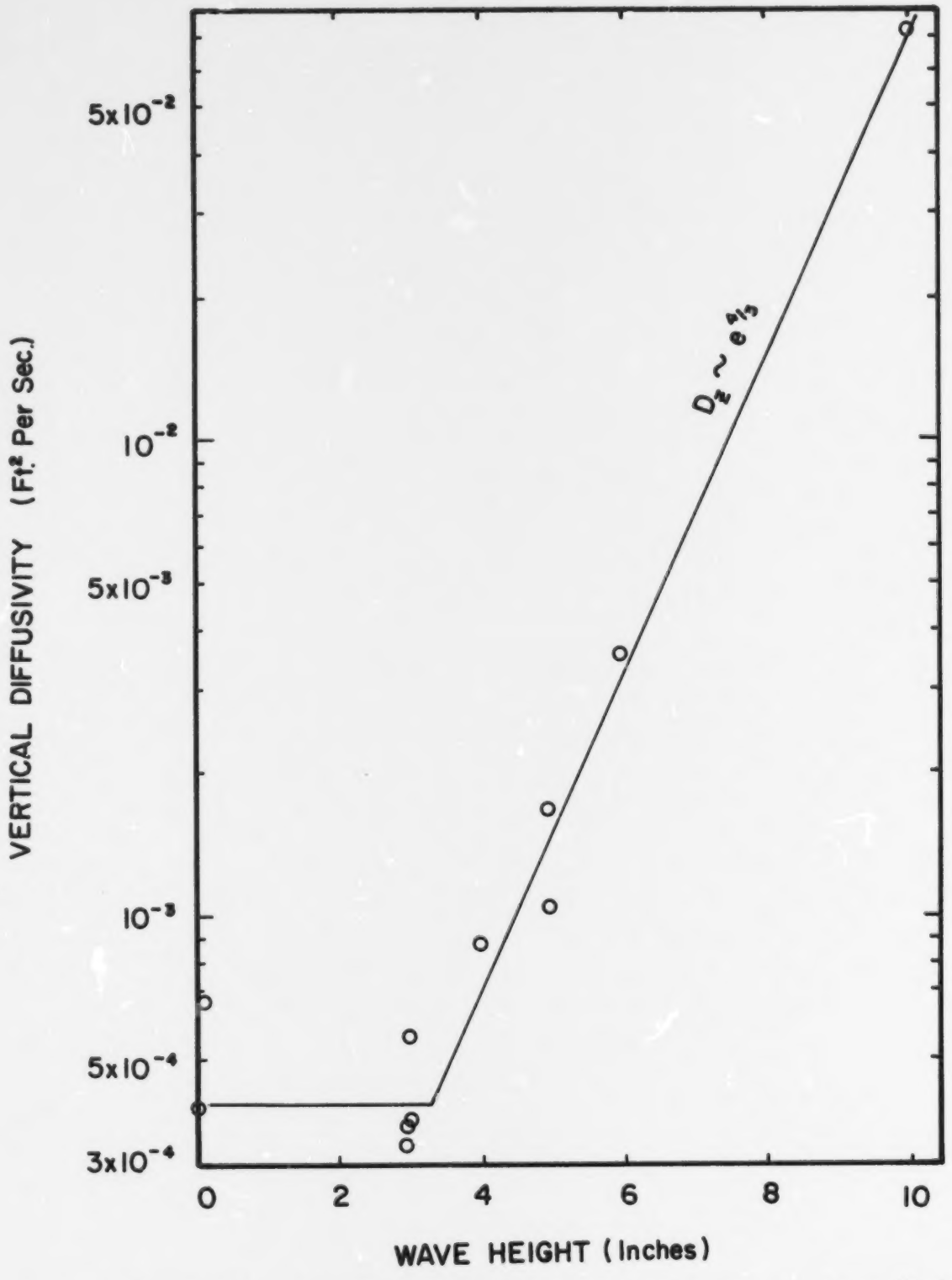

Fig. 4-10 Vertical Dispersion Coefficient vs. Wave Height

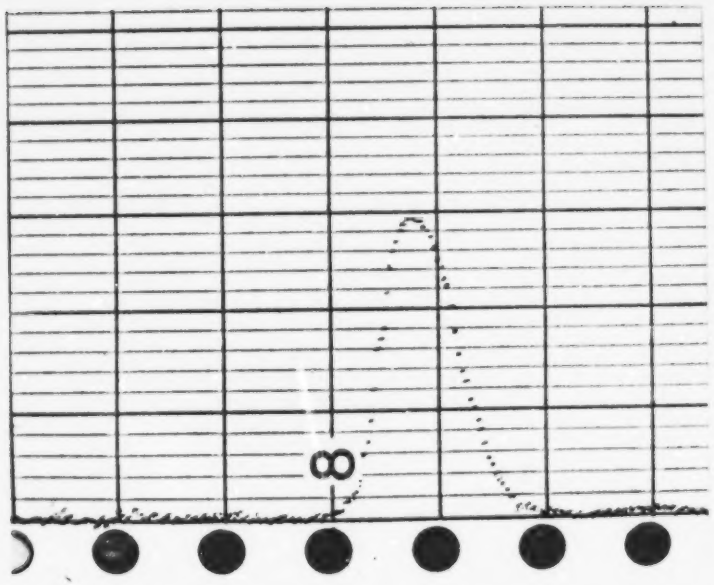

Fig. 4-11 Strip Chart Of Fluorescence Profile For Lateral Traverse

the peak ordinate, the width of the curve is one standard deviation; at 60.7%, two standard deviations, and at 4.5%, the curve is five standard deviations wide.

Assuming normal distribution of the concentration , the standard deviation may be estimated as one-half of the width of the concentration vs. distance curve at the level at which $c = 0.607\ c_{max}$.

The curve on the recorder chart is in fluorescence units rather than in units of concentration. These two values are related by:

$$c = kF^{0.9} \qquad (3\text{-}3)$$

so that at $c = 0.607\ c_{max}$, we have $F = 0.574\ F_{max}$, and the standard deviation is calculated as follows:

1. Measure the width of the trace of the fluorometer output on the strip chart at the value where $F = 0.574\ F_{max}$;
2. Multiply measurement (1) by the chart speed and by the boat velocity to get the width in units of distance in the plume;
3. The result of step (2) is two standard deviations, 2σ. (see figure 4-12).

The coefficient of lateral dispersion, D_y, was calculated by plotting σ vs. $t^{1/2}$ as shown in figure 4-13. The slope of the line of best fit through the origin and the points is $\sqrt{2\ D_y}$. The results of the calculations are shown in Table 4-5.

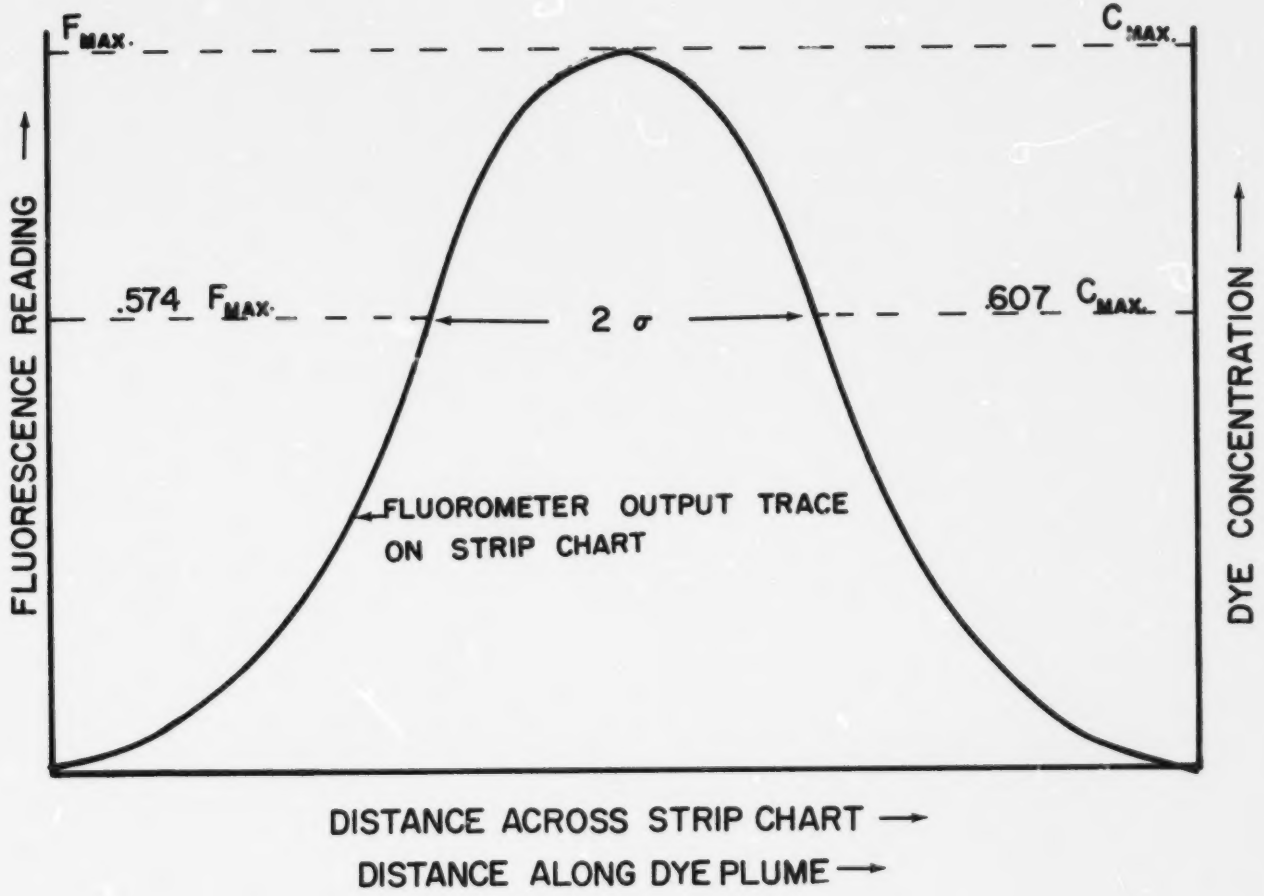

Fig. 4-12 Method Of Estimating Standard Deviation (σ) From Fluorescence Profile

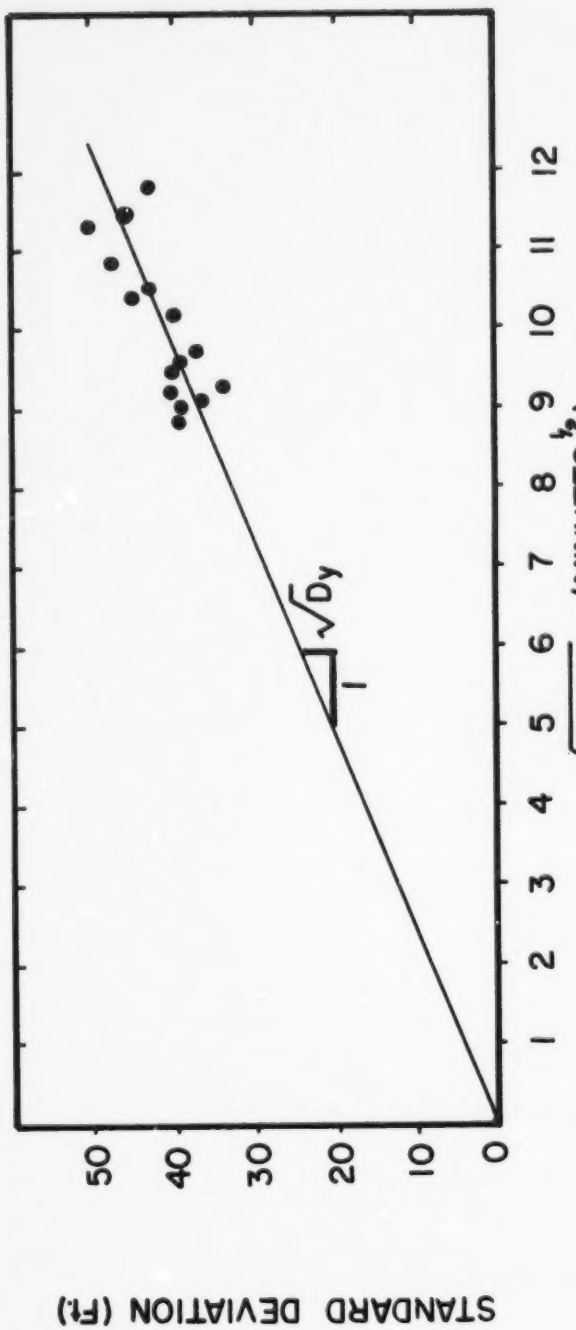

Fig. 4-13 Graphical Method of Calculating Dy

TEST	H(in)	T(sec)	U_s(ft/sec)	D_y(ft^2/sec)	REMARKS
H1	0	-	.13	.052	
H2	6"	1.2	.60	.117	Whitecaps
H3	Ripples	-	.18	.066	
H4	6"	1.2	.63	.098	Whitecaps
H5	5"	1.0	.25	.068	
H6	Ripples	-	.13	.060	
H7	5"	1.0	.43	.075	
H8	10"	1.4	.53	.133	Whitecaps

TABLE 4-5 LATERAL DISPERSION TESTS

In figure 4-14, D_y is plotted against U_s. There is quite a bit of scatter, but the lateral diffusivity generally increases with the surface current in the relation $D_y \sim U_s^{0.4}$.

In Lake Huron studies, Csanady (1963) found no relationship between D_y and U_s, but it is noted that his data show no relationship between wind and current. Apparently the currents at the site of his study are affected by other factors more than by the wind.

Masch (1962), from measurements in a laboratory flume, found an exponential relationship: $D_y \sim U_s^{3.3}$. The difference between his 3.3 power and 0.4 power shown in figure 4-14 may result from the effects of the flume boundaries and the lack of vertical mixing in his experiment which was conducted with floating particles.

Figure 4-15 is a plot of D_y vs. D_z. The vertical coefficient of dispersion varies from 0.00039 to 0.072 sq. ft. per second while the lateral coefficient varies from 0.060 to 0.133 sq. ft. per second. The data are represented by the relationship $D_y \sim D_z^{0.15}$. This seems to indicate that both coefficients are functions of the same parameters of eddy diffusion but that they are related to these parameters in a slightly different manner.

4-8 Longitudinal Dispersion

As a cloud of dispersing dye grows in size and decreases in concentration, its outline becomes indistinct and difficult to locate. The

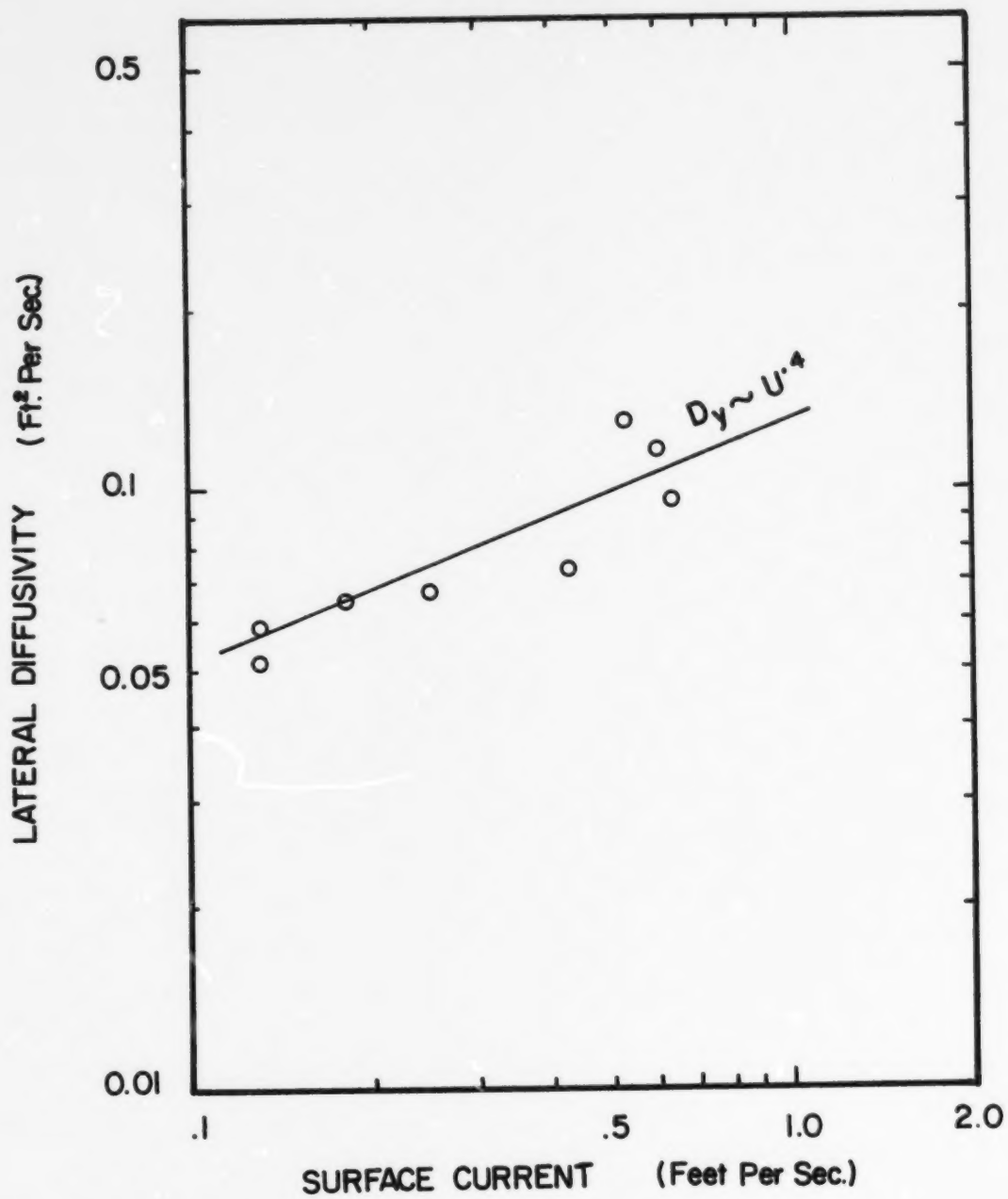

Fig. 4-14 Lateral Dispersion Coefficient vs. Surface Current Velocity

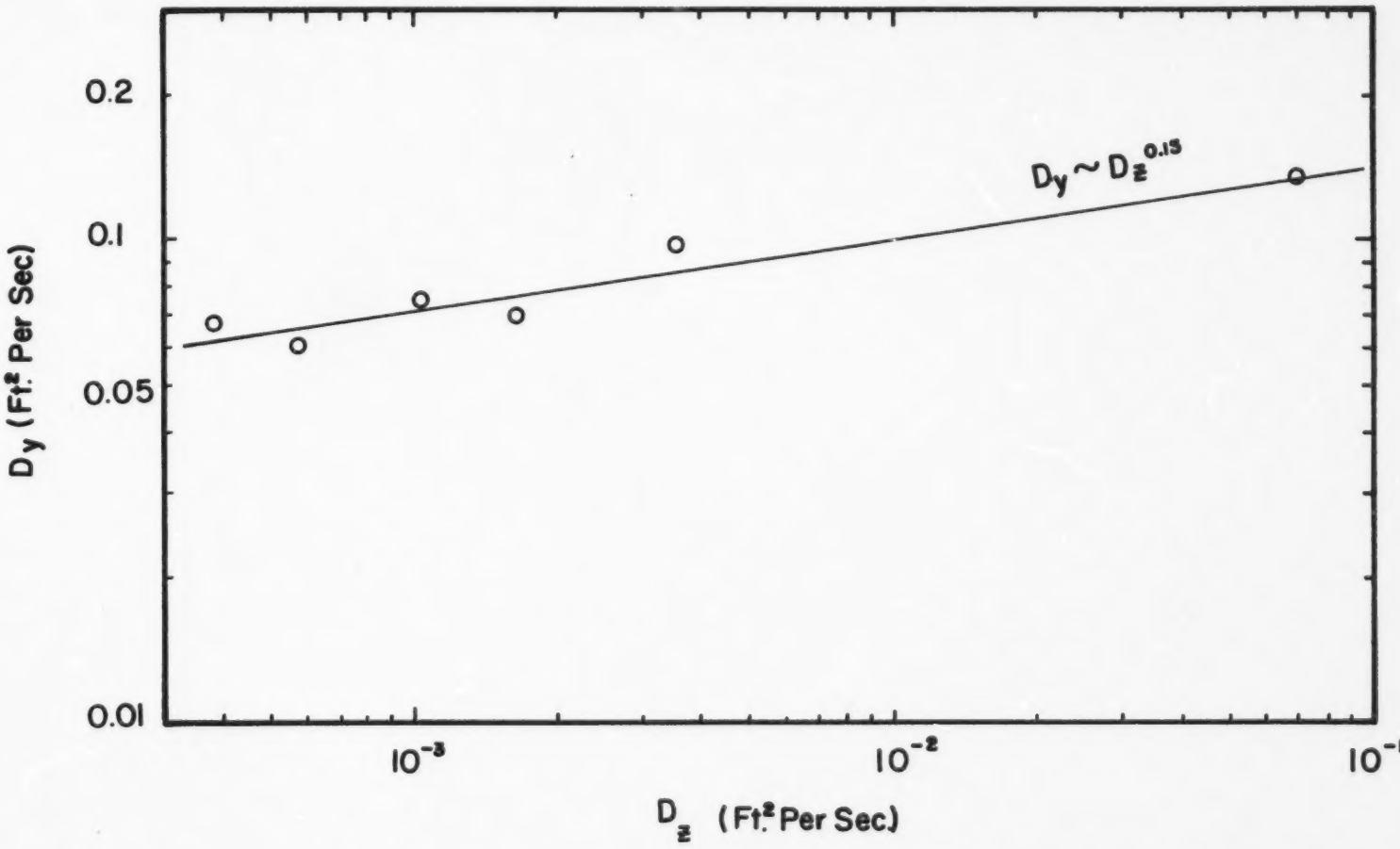

Fig. 4-15 Relationship Between Lateral And Vertical Coefficients Of Dispersion

effect of eddies larger than the cloud sometimes results in a warped, curving or crooked cloud shape. Since the boat cannot be made to follow the centerline of the cloud, the record of the fluorometer output during a longitudinal traverse cannot be analyzed in the same manner as that of a lateral traverse. Figure 4-16 is a photograph of a typical strip chart of fluorometer output during a longitudinal traverse of the cloud.

In figure 4-17, a curving cloud is sketched with its centerline (or line of maximum lateral concentration) shown as a broken line. The straight solid line represents the path of the boat making a longitudinal traverse. Beside the sketch is a graph of the concentration in the cloud. The concentration along the centerline is shown dotted, and that along the boat's path is shown as a solid line. Obviously, the chart of the concentration along the boat's path cannot be used to calculate the dispersion coefficient in the same way it was used for the lateral coefficient. At best, the chart can be used to estimate the length of the cloud. If the length is assumed to be six standard deviations (containing 99.8% of the material) a dispersion coefficient can be calculated. In this manner the values of the longitudinal dispersion coefficient, D_x, were estimated from the data in Table 4-6 to be 2.1 sq. ft. per second in a 6" wave and 36 fpm surface current condition and 3.1 sq. ft. per second in a calm and 11 fpm surface current condition.

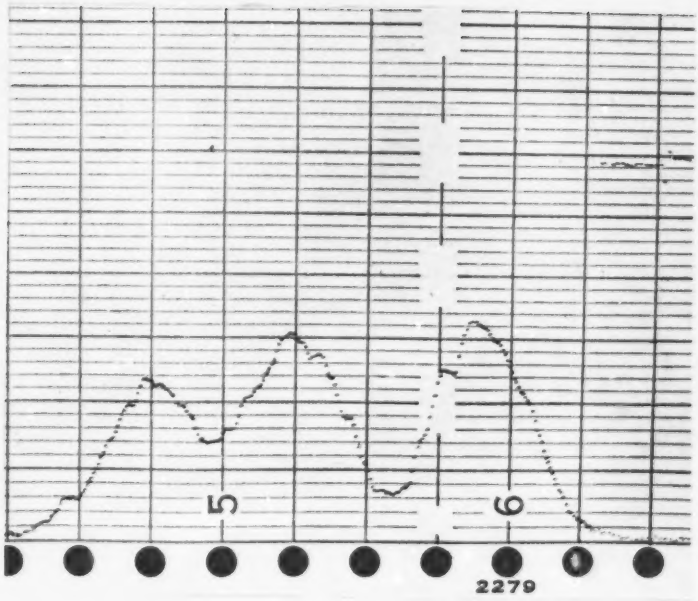

Fig. 4-16 Strip Chart Of Fluorescence Profile For Longitudinal Traverse

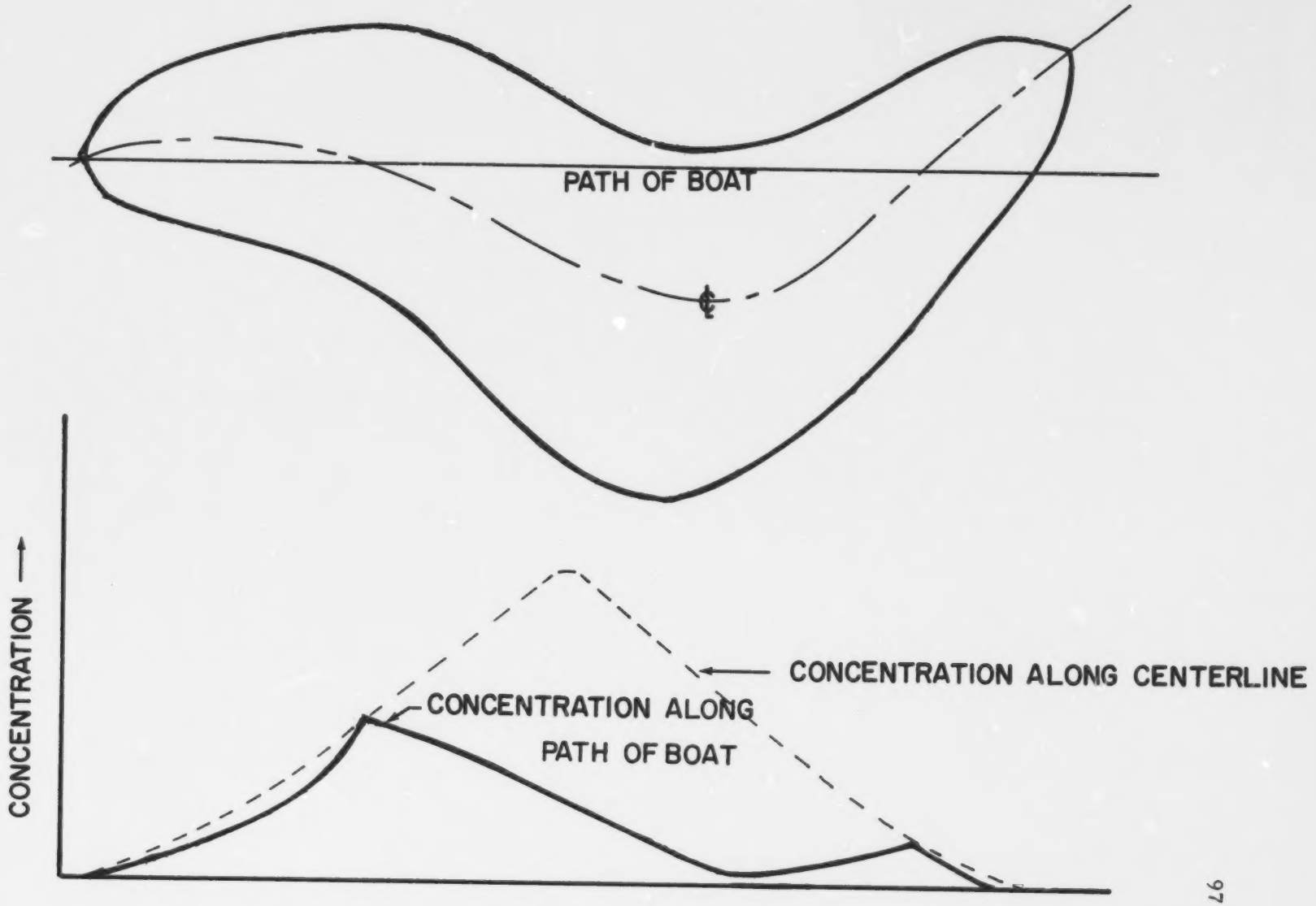

Fig. 4-17 Concentration Profile In Curving Cloud

TABLE 4-6

Wave Height (inches)	Surface Current (ft. per min.)	Time (hr.)	Lateral Length (ft.)	Longitudinal Length (ft.)	Length/ Width
6	36	1	170	740	4.3
Calm	11	4	260	1800	6.9

Dimensions of dye clouds on two occasions with different surface conditions are shown in Table 4-6. Longitudinal dispersion decreases with an increase in wave height and surface current, but the lateral dispersion was previously shown to behave in an opposite manner. This causes the length-to-width ratio to decrease as the sea state increases. This agrees with the findings of Katz, et al (1965) that the rate of elongation decreases as the wind velocity and sea state increase. It also supports the findings of Bowden (1964) that the longitudinal and vertical coefficients of dispersion are inversely proportional. These findings do not support equation (2-28), proposed by Csanady, which gives a solution for the longitudinal dispersion coefficient that increases with the wind velocity.

From visual estimates of the cloud dimensions during the first thirty to forty minutes of its growth, the extreme dimension in the longitudinal direction usually appeared to be 5 to 10 times the concurrent lateral dimension. It was obvious that in very weak currents the longitudinal and lateral dimensions were more nearly equal than they

were in strong currents. When the surface current is very weak, there is little shear and little change in velocity with depth. For this reason, the shear flow mixing is much less pronounced, and the difference in dispersion coefficients for the lateral and longitudinal directions (being due primarily to the shear flow mixing) is much less. As the current increases, there is a greater velocity gradient with depth, and the shear flow mixing increases causing the cloud to elongate in the longitudinal direction. The increase in the surface current velocity is, however, accompanied by an increase in the energy in the wave spectrum and an increase in turbulence. As was shown previously, this increase in turbulence causes an increase in the vertical dispersion coefficient, and the increase in the rate of vertical mixing reduces the shear flow mixing effect. Since the vertical dispersion was found to be constant over the low range of surface conditions, the elongation should reach a maximum at some condition near the upper end of this range. From this point it will decrease as the increasing vertical mixing reduces the shear flow mixing.

CHAPTER 5

CONCLUSIONS

The dominant mechanism for dispersion in a lake is the spatial variation in the velocity of the currents. The variation may be in direction or in magnitude. Assuming no boundary effects, when the currents are wind-driven and are in equilibrium with a steady wind, the current velocity is a maximum at the water surface and decreases with depth. This causes the cloud to be transported at different rates at different depths and, in this situation, vertical dispersion increases the longitudinal dispersion. This shear flow mixing accounts for the observations in which the longitudinal dispersion was five to ten times that in the lateral direction.

The velocity may also change direction with depth causing the cloud to be transported in different directions at different levels. In this situation, vertical dispersion increases the lateral dispersion as well as the longitudinal - such a situation is observed when the wind direction changes. There is a long lag before the viscous shear overcomes the inertia of the water and causes the currents to align themselves with the wind.

Turbulence is also a very significant dispersion mechanism. As was explained previously, the random turbulent fluctuations in velocity cause diffusion in a manner analogous to molecular diffusion.

This eddy diffusion is a function of the energy transmitted to the water from the wind which blows over the surface of the water.

Based on the experimental investigation reported herein, the following conclusions have been reached:

1. During the time interval from one to six hours, the peak concentration was found to decrease as the minus 2.5 power of time. This rate occurred at sites with very different geometric characteristics; it occurred over a range of differing ambient conditions; it occurred over a range of different initial concentrations; and it occurred in two-dimensional dispersion of a dye having a very low density as well as in three-dimensional dispersion of a dye having a density equal to that of the receiving water. The empirical formula thus derived is:

$$C/C_o = \alpha t^{-2.5} \qquad (4\text{-}11)$$

The dilution coefficient, α, is included to account for the turbulence and is found to be related to the surface current by the equation.

$$\alpha \sim K_c U_s^{-3} \qquad (4\text{-}12)$$

where K_c is a factor applied to account for different

surface conditions. K_c was found to be 0.78 when whitecaps are present and to be 1.00 for the "no whitecap" condition. This factor is necessary because when the waves begin to break, the surface current represents a smaller portion of the total energy in the system. The dilution coefficient is related to the energy transmitted to the water by the wind blowing over its surface.

2. In equilibrium conditions with a steady wind, the surface current appears to be a good parameter for the energy in the wave spectrum and thus for the turbulent diffusivity. The velocity of the surface current must be corrected by a factor when the waves begin to break as was noted above. The velocity of the surface current is a good parameter for describing both the lateral coefficient of dispersion and the dilution coefficient. The vertical coefficient of dispersion is better correlated with the wave height.

3. Comparative values of the three dispersion coefficients are (in units of sq. ft. per second):

Wave	Longitudinal	Lateral	Vertical
Ripple	3	0.06	0.0004
6"	2	0.11	0.0035
10"	-	0.13	0.0720

The vertical and lateral coefficients of dispersion increase with the energy in the wave spectrum but in a different

manner so that:

$$D_y \sim D_z^{0.15}$$

The longitudinal coefficient of dispersion is greater than the lateral coefficient because of (and by the amount of) the shear flow mixing. The longitudinal coefficient of dispersion decreases as the vertical coefficient increases because the shear flow mixing, which makes up the larger part of the longitudinal coefficient, is reduced by increased vertical mixing. The vertical coefficient is essentially constant until the wave height reaches approximately three inches and then increases very rapidly with wave height. Cloud elongation thus is a maximum at this wave height and decreases as the vertical coefficient increases.

4. In a wind-generated current, the velocity gradient is very steep near the surface and diminishes with depth. The one-seventh power law fits the data reasonably well. The gradient of the velocity relative to the surface current velocity appears to be independent of the ambient conditions.

CHAPTER 6

RECOMMENDATIONS FOR FUTURE STUDY

1. Since the velocity distribution is so important to the mixing process, it should be studied more carefully with more accurate measuring devices and under a wide range of conditions.

2. The velocity of the surface current appears to be an easily measured parameter which is well correlated with α, the turbulence coefficient in the dilution rate equation (4-11). More study should be directed toward establishing the relationship between α and U_s so that the time rate of diminution of peak concentration can be predicted by using the velocity of the surface current.

3. This investigation limited dilution times to six hours. The experiments should be conducted over a much longer period of time to determine whether the $t^{-2.5}$ relation holds indefinitely.

4. Equation (4-8) indicates that the eddy diffusivity is proportional to the 6/5 power of the distance to the mass center. This should be investigated more thoroughly in a system of wind-generated currents.

APPENDIX A

Velocity Distribution Test Data

VELOCITY DISTRIBUTION TESTS

Surface Current (Fps) at Various Depths

Test	Date	Waves	Surface	3'	5'	8'	10'	15'	25'	35'
U-1	3-3-66	14"	1.00		0.43		0.35	0.30		
U-2	3-4-66	12"	0.87		0.28		0.24	0.23		
U-3	3-8-66	12"	0.78	0.51		0.27		0.24	0.21	0.11
U-4	6-16-66	5"	0.34				0.10			0.05
U-5	6-17-66	5"	0.31				0.13			0.07
U-6	6-28-66	5"	0.25				0.07			0.09
U-7 A	7-12-66	5"	0.37	0.23			0.17			0.13
U-7 B	7-12-66	8"	0.72				0.36			0.27

APPENDIX B

Horizontal Dispersion Test Data

HORIZONTAL DISPERSION TEST NO. H-1

DATE 5-30-66 SITE 1 DYE 100 mg.

LAKE SURFACE: U_s 8 fpm E ; H Ripple in. ; T - sec.

TIME (min)	BOAT VELOCITY (fpm.)	INTAKE DEPTH (ft.)	FLUOR SCALE	TEMP (^{o}C)	MAX F	CLOUD WIDTH (ft.)	STANDARD DEVIATION (ft.)
105	260	1.5	3x	26	23	150	26
113	260	1.5	10x	26	50	152	26
120	260	1.5	3x	26	24	158	27

HORIZONTAL DISPERSION TEST NO. H-2

DATE 5-30-66 SITE 1 DYE 75 mg.

LAKE SURFACE: U_s 36 fpm E ; H 6 in. ; T 1.2 sec.

TIME (min)	BOAT VELOCITY (fpm)	INTAKE DEPTH (ft.)	FLUOR SCALE	TEMP (°C)	MAX F	CLOUD WIDTH (ft.)	STANDARD DEVIATION (ft.)
LATERAL							
68	265	1.5	3x	26	34	170	31
70	265	↓	↓	↓	33	175	31
72	260	↓	↓	↓	32	190	32
74	265	↓	↓	↓	28	185	32
96	270	↓	10x	↓	53	208	37
97	265	↓	10x	↓	46	202	36
LONGITUDINAL		↓					
65	280	1.5	3x	26	34	740	130
79	210	↓	↓	↓	26	725	120
92	280	↓	↓	↓	18	840	140

HORIZONTAL DISPERSION TEST NO. H-3

DATE 5-31-66 SITE 1 DYE 75 mg.

LAKE SURFACE: U_s 11 fpm W ; H Ripple in. ; T sec.

TIME (min)	BOAT VELOCITY (fpm)	INTAKE DEPTH (ft.)	FLUOR SCALE	TEMP (°C)	MAX F	CLOUD WIDTH (ft.)	STANDARD DEVIATION (ft.)
LATERAL							
60	230	1.0	1x	26	62	136	22
62	220		1x		96	143	22
122	230		10x		91	176	31
226	220		30x		58	260	43
LONGITUDINAL							
250	220	1.0	30x	26	38	1750	290

HORIZONTAL DISPERSION TEST NO. H-4

DATE 6-2-66 SITE 1 DYE 75 mg.

LAKE SURFACE: U_s 38 fpm SSE ; H 6 in. ; T 1.2 sec.

TIME (min)	BOAT VELOCITY (fpm)	INTAKE DEPTH (ft.)	FLUOR SCALE	TEMP (°C)	MAX F	CLOUD WIDTH (ft.)	STANDARD DEVIATION (ft.)
LATERAL							
65	240	1.5	1x	25	26	146	27
100	235	↓	3x	↓	35	188	35
101	230	↓	↓	↓	28	190	35
106	235	↓	↓	↓	26	185	35
180	240	↓	10x	↓	22	254	46
182	240	↓	10x	↓	20	242	44

HORIZONTAL DISPERSION TEST NO. H-5

DATE 6-28-66 SITE 1 DYE 100 mg.

LAKE SURFACE: U_s 15 fpm E ; H 5 in. ; T 1.0 sec.

TIME (min)	BOAT VELOCITY (fpm)	INTAKE DEPTH (ft.)	FLUOR SCALE	TEMP (°C)	MAX F	CLOUD WIDTH (ft.)	STANDARD DEVIATION (ft.)
LATERAL							
228	280	1.0	10x	28.5	26	220	43
232	300	↓	↓	↓	17	195	36
234	↓	↓	↓	↓	20	225	43
236	↓	↓	↓	↓	18	198	36
238	↓	↓	↓	↓	20	205	43
240	↓	↓	↓	↓	16	200	43
251	290	↓	30x	28.6	92	247	46
254	300	↓	↓	28.7	86	240	45
257	285	↓	↓	↓	78	249	47
259	280	↓	↓	↓	61	243	47
262	300	↓	↓	↓	37	239	46
265	290	↓	↓	↓	69	257	48

HORIZONTAL DISPERSION TEST NO. H-6

DATE 6-29-66 SITE 1 DYE 100 mg.

LAKE SURFACE: U_s 8 fpm S ; H Ripple in. ; T - sec.

TIME (min)	BOAT VELOCITY (fpm)	INTAKE DEPTH (ft.)	FLUOR SCALE	TEMP (^{o}C)	MAX F	CLOUD WIDTH (ft.)	STANDARD DEVIATION (ft.)
178	260	1.0	10x	28.5	60	195	34
181	↓	↓	↓	↓	48	214	38
183	↓	↓	↓	↓	40	200	36

HORIZONTAL DISPERSION TEST NO. H-7

DATE 7-12-66 SITE 1 DYE 150 mg.

LAKE SURFACE: U_s 26 fpm SSE ; H 5 in. ; T 1.0 sec.

TIME (min)	BOAT VELOCITY (fpm)	INTAKE DEPTH (ft.)	FLUOR SCALE	TEMP (°C)	MAX F	CLOUD WIDTH (ft.)	STANDARD DEVIATION (ft.)
71	260	1.0	3x	28.7	14	150	26
74	260	↓	↓	↓	28	144	27
76	300	↓	↓	↓	18	148	26
79	300	↓	10x	↓	84	160	26
80	260	↓	↓	↓	74	170	27
86	265	↓	↓	↓	74	170	27
87	260	↓	↓	↓	72	175	28

HORIZONTAL DISPERSION TEST NO. H-8

DATE 9-13-66 SITE 1 DYE 75 mg.

LAKE SURFACE: U_s 32 fpm SE ; H 10 in. ; T 1.4 sec.

TIME (min)	BOAT VELOCITY (fpm)	INTAKE DEPTH (ft.)	FLUOR SCALE	TEMP (^{o}C)	MAX F	CLOUD WIDTH (ft.)	STANDARD DEVIATION (ft.)
79	300	2.0	3x	28.7	22	212	39
81	290				21	215	39
83	300				21	210	39
85	295				19	215	40
88	300				19	215	41
90	300				17	220	41
108	290		10x		30	247	46
110	295				30	255	45
112	300				27	254	45
125	265				24	300	50
128	275				23	250	50
131	300				23	270	51

APPENDIX C

Vertical Dispersion Test Data

VERTICAL DISPERSION TEST NO. V-1

DATE 5-31-66 SITE 1 DYE 75 mg.

LAKE SURFACE: U_s 11 fpm W ; H Ripple in. ; T sec.

TIME (min)	FLUOR SCALE	0	1'	2'	3'	4'	5'	6'	7'
71	10x	60							
71	30x	-	94	34	11	6	5	1	1
114	30x	25	16	12	85	3.5	2	1	1

REMARKS: Discrete Sampler

VERTICAL DISPERSION TEST NO. V-2

DATE 6-2-66 SITE 1 DYE 75 mg.

LAKE SURFACE: U_s 38 fpm SSE ; H 6 in. ; T 1.2 sec.

TIME (min)	FLUOR SCALE	0	2 1/2'	5	7 1/2'	10	12 1/2'	15	17 1/2'	20'
153	30x	30	28	28	27	12	7	1	1	1

		0	1'	2'	3'	4'	5'
82	30x	30	29	28.5	28	27	24

REMARKS: 153 min. test made with continuous flow apparatus

82 min. test made with discrete sampling procedure

VERTICAL DISPERSION TEST NO. V-3

DATE 6-28-66 SITE 1 DYE 100 mg.

LAKE SURFACE: U_s 15 fpm E ; H 5 in. ; T 1.0 sec.

TIME (min)	FLUOR SCALE	0	1'	2'	3'	4'	5'	6'	7'	8'	9'
55	1x	34	32	28	24	22	11	2	1	0	0
93	10x	95	90	88	81	81	50	22	9	6	2
117	30x	66	65	64	63	63	56	50	31	9	4
175	30x	66	64	62	60	62	58	47	29	8	6

REMARKS: Discrete Sampler

VERTICAL DISPERSION TEST NO. V-4

DATE 6-29-66 SITE 1 DYE 100 mg.

LAKE SURFACE: U_s 8 fpm S ; H Ripple in. ; T sec.

TIME (min)	FLUOR SCALE	0	1'	2'	3'	4'	5'	6'	7'	8'	9'
62	3x	88	84	64	17	9	1	0.5	0	0	0
115	10x	70	65	39	30	27	12	2	0	0	0
155	10x	45	40	35	27.5	18	15	8	2	0	0
195	30x	62	60	51	44	29	14	9	7	3.5	2

REMARKS: Discrete Sampler

VERTICAL DISPERSION TEST NO. V-5

DATE 7-12-66 SITE 1 DYE 150 mg.

LAKE SURFACE: U_s 26 fpm SSE ; H 5 in. ; T 1.0 sec.

TIME (min)	FLUOR SCALE	0	1'	2'	3'	4'	5'	6'	7'	8'	9'	15'
137	10x	81	75	72	51	44	30	17	15	12	7.5	1

REMARKS: Discrete Sampler

VERTICAL DISPERSION TEST NO. V-6

DATE 7-13-66 SITE 1 DYE 75 mg.

LAKE SURFACE: U_s 32 fpm SE H 10 in.; T 1.4 sec.

TIME (min)	FLUOR SCALE	0	1'	2'	3'	4'	5'	6'	7'	8'	9'	15'
93	30x	50	49	50	40	39	37	36	31	30	30	9

REMARKS: Discrete Sampler

VERTICAL DISPERSTION TEST NO. V-7

DATE 7-19-66 SITE 1 DYE 100 mg.

LAKE SURFACE: U_s 16 fpm SSW ; H 3 in. ; T 0.9 sec.

TIME (min)	FLUOR SCALE	0	1'	2'	3'	4'	5'	6'	7'	8'	9'
61	3x	54	52	26.5	18	6	2.5	2.5	0	0	0
165	30x	99	96	39	20	9	5	3	2	1	1
277	30x	24	22	19	17	12	5	3	2	1	1

REMARKS: Discrete Sampler

VERTICAL DISPERSION TEST NO. V-8

DATE 7-19-66 SITE 1 DYE 40 mg.

LAKE SURFACE: U_s 17 fpm SSW ; H 3 in. ; T 0.9 sec.

TIME (min)	FLUOR SCALE	0	1'	2'	3'	4'	5'	6'	7'	8'	9'
73	10x	63	61	52	39	20	8	1	0	0	0
142	30x	68	66	62	35	17	5	3	2	1	1

REMARKS: Discrete Sampler

VERTICAL DISPERSION TEST NO. V-9

DATE 7-20-66 SITE 2 DYE 100 mg.

LAKE SURFACE: U_s 18 fpm S ; H 3 in. ; T 0.9 sec.

TIME (min)	FLUOR SCALE	0	1'	2'	3'	4'	5'	6'	7'	8'	9'
121	10x	40	38	35.5	17	1	.5	0.	0	0	0
183	30x	56	53.5	51.5	41	16	10	3	2	1	1
250	30x	32	30	30	23	14.5	3	2	1	1	1
295	30x	21	20	20	17.5	8	3	2	1	1	1

REMARKS: Discrete Sampler

VERTICAL DISPERSION TEST NO. V-10

DATE 7-21-66 SITE 2 DYE 100 mg.

LAKE SURFACE: U_s 19 fpm SSW; H 4 in.; T 1.0 sec.

TIME (min)	FLUOR SCALE	0	1'	2'	3'	4'	5'	6'	7'	8'	9'
69	3x	47	43	38	34	14	3.5	1.5	1	0	0
122	10x	38	36	36	26	21	8	--	3	2	2
185	30x	20	14.5	9	5	2	2	2	2	2	2

REMARKS: Discrete Sampler

VERTICAL DISPERSION TEST NO. V-11

DATE 7-22-66 SITE 3 DYE 25 mg.

LAKE SURFACE: U_s 12 fpm NW ; H Ripples in.; T — sec.

TIME (min)	FLUOR SCALE	0	1'	2'	3'	4'	5'	6'	7'	8'	9'
95.5	30x	98	74	48.5	13	12	4	2	1	0	0
153.5	30x	61	47	46	35	17	10	6	3.5	2	2
212.5	30x	21	17	17	13	4.5	2	2	2	2	2

REMARKS: Discrete Sampler

APPENDIX D

Dilution Rate Test Data

DILUTION RATE TEST NO. P-1

DATE 5-30-66 SITE 1 DYE 75 mg.

LAKE SURFACE: U_s 36 fpm E ; H 6 in. ; T 1.2 sec.

TIME(min)	65	70	79	92	97
F	44	33	26	18	46
SCALE	3x	3x	3x	3x	10x
TEMP(^{o}C)	26	26	26	26	26

DILUTION RATE TEST NO. P-2

DATE 7-13-66 SITE 1 DYE 75 mg.

LAKE SURFACE: U_s 32 fpm SE ; H 10 in. ; T 1.4 sec.

TIME(min)	79	89	119	128	133	141
F	23	20	26	24	20	18
SCALE	3x	3x	10x	10x	10x	10x
TEMP(^{o}C)	28.7	28.7	28.7	28.7	28.7	28.7

DILUTION RATE TEST NO. P-3

DATE 7-19-66 SITE 1 DYE 100 mg.

LAKE SURFACE: U_s 16 fpm SSW ; H 3 in. ; T 0.9 sec.

TIME(min)	70	111	135	157	169
F	68	72	38	28	23
SCALE	1x	3x	3x	3x	3x
TEMP(^{o}C)	30	30	30	30	30

TIME(min)	226	277	296	320
F	26	18	68	60
SCALE	10x	10x	30x	30x
TEMP(^{o}C)	30	30	30	30

DILUTION RATE TEST NO. P-4

DATE 7-19-66 SITE 1 DYE 40 mg.

LAKE SURFACE: U_s 17 fpm SSW ; H 3 in. ; T 0.9 sec.

TIME(min)	67	73	98	122	142
F	74	65	95	61	39
SCALE	3x	3x	10x	10x	10x
TEMP(^{o}C)	30	30	30	30	30

DILUTION RATE TEST NO. P-5

DATE 7-20-66 SITE 2 DYE 100 mg.

LAKE SURFACE: U_s 18 fpm ; H 3 in. ; T 0.9 sec.

TIME(min)	60	88	97	120	127	153
F	51	30	71	43	39	86
SCALE	1x	1x	3x	3x	3x	10x
TEMP(^{o}C)	30	30	30	30	30	30
TIME(min)	185	233	250	267	302	319
F	43	28	18	78	60	50
SCALE	10x	10x	10x	30x	30x	30x
TEMP(^{o}C)	30	30	30	30	30	30

DILUTION RATE TEST NO. P-6

DATE 7-21-66 SITE 2 DYE 100 mg.

LAKE SURFACE: U_s 19 fpm SSW ; H 4 in. ; T 1.0 sec.

TIME (min)	98	120	150	184	235	270
F	55	29	45	28	71	63
SCALE	3x	3x	10x	10x	30x	30x
TEMP (^{o}C)	30.3	30.3	30.3	30.3	30.3	30.3

DILUTION RATE TEST NO. P-7

DATE 7-22-66 SITE 3 DYE 25 mg.

LAKE SURFACE: U_s 12 fpm * ; H Ripple in. ; T — sec.

TIME(min)	95	120	155	179	220	244	301
F	48	25	45	30	19	73	40
SCALE	3x	3x	10x	10x	10x	30x	30x
TEMP(^{o}C)	31.3	31.3	31.3	31.3	31.3	31.3	31.3

REMARKS: * At 120 min. surface current reversed direction from 15 fpm N W to 12 fpm S E

DILUTION RATE TEST NO. P-8

DATE 7-25-66 SITE 3 DYE 25 mg.

LAKE SURFACE: U_s 13 fpm SE ; H Ripples in. ; T — sec.

TIME(min)	67	192	220	246
F	42	25	20	59
SCALE	1x	10x	10x	30x
TEMP(^{o}C)	31.8	32.0	32.0	32.0

DILUTION RATE TEST NO. P-9

DATE 8-18-66 SITE 1 DYE 100 mg.

LAKE SURFACE: U_s 16 fpm N ; H Ripple in. ; T -- sec.

TIME	62	68	98	105	116
F	63	43	42	34	25
SCALE	1x	1x	3x	3x	3x
TEMP(°C)	30	--	--	--	30

TIME	136	172	196	218
F	57	28	20	15
SCALE	10x	10x	10x	10x
TEMP	--	30	--	30

REMARKS: Dye was mixed in one liter of methanol. Regular thermometer inoperative-used mercury thermometer to check lake water temperature. At 90 min., speedboat passed through dye cloud at high speed.

BIBLIOGRAPHY

Baines, W. D. and D. J. Knapp (1965) Wind Driven Water Currents, J. Hydraulics Div., Amer. Soc. of Civ. Engrs., 91, HY 2, March.

Batchelor, G. K. (1952) Diffusion in a Field of Homogeneous Turbulence. II The Relative Motion of Particles. Proc. Camb. Phil Soc., 48, 345.

Bowden, K. F. (1965) Horizontal Mixing in the Sea Due to a Shearing Current. J. of Fluid Mech., 21, 83-96.

Buchanan, T. J. (1964) Time of Travel of Soluble Contaminants in Streams. J. Sanitary Engr. Div., Amer. Soc. of Civ. Engrs., 90, SA 3, 1-12.

Carslaw, H. S. and V. C. Jaeger (1959) Conduction of Heat in Solids, 2nd ed., Clarendon Press.

Cramer, H. E. (1959) Engineering Estimates of Atmospheric Dispersal Capacity. Industrial Hygene Journal, 20, 3, June, 183-189.

Csanady, G. T. (1963) Turbulent Diffusion in Lake Huron. J. of Fluid Mech. 17, 3, 360-384.

Csanady, G. T. (1966) Accelerated Diffusion in the Skewed Shear Flow of Large Currents. J. of Geophys. Res., 171, 2, 411-420.

Deacon, E. L. (1962) Aerodynamic Roughness of the Sea, J. Geophys. Res., 67, 8, 3167-72.

Diachishin, A. N. (1963) Dye Dispersion Studies. J. of San. Engr. Div., Amer. Soc. of Civ. Engr., 89, SA 1, 29-50.

Dobbins, W. E. (1965) Diffusion and Mixing. J. of Boston Soc. of Civ. Engr., 52, 2, 108-128

Elder, J. W. (1959) The Dispersion of Marked Fluid in Turbulent Shear Flow. J. of Fluid Mech., 5, 544-560.

Feuerstein, D. L. and R. E. Selleck (1963) Fluorescent Tracers for Dispersion Measurements. J. of San Engr. Div., Amer. Soc. of Civ. Engr., 89, SA 4, Aug.

Foxworthy, J. E., et al, (1966) Dispersion of a Surface Waste Field in the Sea, J. Water Pol'n. Control Fed, 38, 7, July, 1170-93.

Frenkiel, F. N., ed. (1962) SYMPOSIUM ON FUNDAMENTAL PROBLEMS IN TURBULENCE AND THEIR RELATION TO GEOPHYSICS, Amer. Geophys. Union, Wash, D. C.

Friedlander, S. K. and L. Topper (1961) Turbulence: Classical Papers on Statistical Theory. Interscience Publishers, Inc., New York. (edited)

Gunnerson, C. G. (1960) Discussion of Eddy Diffusion in Homogeneous Turbulence. J. Hyd. Div., Amer. Soc. of Civ. Engr., 85, HY 4, 101-109.

Haines, D. A. and R. A. Bryson (1961) An Empirical Study of Wind Factor in Lake Mendota, Limnology and Oceanography, 6, 3, July, 356-363.

Hinze, J. O. (1959) Turbulence. McGraw-Hill Book Co., New York.

Ichiye, T. (1962) Studies of Turbulent Diffusion of Dye Patches in the Ocean, J. of Geophys. Res. 67,8, 3213-16.

Ippen, A. T. and F. Raichlen (1957) Turbulence in Civil Engineering: Measurements in Free Surface Streams. J. Hyd. Div., Amer. Soc. of Civ. Engr., 83, HY5, 10.

Johnson, J. W. (1950) Relation Between Wind and Waves--Abbots Lagoon, Cal. Trans. Amer. Geophys. Union, 31, 3, 386-392.

Johnson, J. W. (1959) The Effect of Wind and Wave Action on the Mixing and Dispersion of Wastes. Hyd. Engr. Lab. Tech. Rep. Series 138, 1, University of Calif., Berkley.

Joseph, J. and H. Sendner (1958) Horizontal Diffusion in the Sea. Dtsch. Hydrogr. Z., 11, 2, 49-77.

Katz, B. et al (1965) Response of Dye Tracers to Sea Surface Conditions. J. of Geophys. Res., 70, 22, 5505-5513.

Keulegan, C. H. (1951) Wind Tides in Small Closed Channels. J. of Res., Natl. Bur. of Stds., 46, 5.

Keulegan, C. H. and V. Brame, Jr. (1960) Fourteenth Progress Report on Model Laws for Density Currents Mixing Effects of Wind Induced Waves., Natl. Bur. of Stds., Rep. 6638.

Kolmogoroff, A. N. (1941) The Local Structure of Turbulence in Incompressible Viscous Fluids for Very Large Reynolds Numbers. Comptes Rendus de l'Academie des Sciences de l'U. R. S. S., 30, 301-305.

Langmuir, I. (1938) Surface Motion of Water Induced by the Wind. Science, 87, 2250, 119-123.

Masch, F. D. (1961) Mixing and Dispersive Action of Waves. Hyd. Engr. Lab. Tech. Rep. Series 138, 6, Univ. of Cal., Berkley.

Munk, W. H. (1947) A Critical Wind Speed for Air-sea Boundary Processes. J. of Mar. Res., VI, 3, 203-218.

Munk, W. H. et al (1949) Diffusion in Bikini Lagoon. Trans. Amer. Geophys. Union, 30, 59-66.

Obukhov, A. M. (1959) Description of Turbulence in terms of Lagrangian Variables. Adv. in Geophys., 6, 113-116.

Okubo, A. (1962) A Review of Theoretical Models for Turbulent Diffusion in the Sea. J. of Oceanogr. Soc. of Japan, 29th annv. vol., 286-319.

Ozmidov, R. V. (1958) On the Calculation of Horizontal Turbulent Diffusion of the Pollutant Patches in the Sea. Doklady Akad. Nauk SSSR 120, 761.

Orlob, G. T. (1958) Eddy Diffusion in Open Channel Flow. San. Engr. Res. Lab., Contr. 19, Univ. of Cal., Berkley.

Orlob, G. T. (1959) Eddy Diffusion in Homogeneous Turbulence. J. Hyd. Div., Amer. Soc. of Civ. Engr., 85, HY 9.

Pai, S. (1957) Viscous Flow Theory. II Turbulent Flow. D. Van Nostrand, Princeton, N. J.

Parker, F. L. (1961) Eddy Diffusion in Reservoirs. J. Hyd. Div., Amer. Soc. of Civ. Engr., 87, HY 3, 151-171.

Patterson, C. C. (1963) The Dispersion of Radionuclides in Open Channel Flow. Tech. Rep. to A. E. C., Env. Health Engr. Res. Lab., Univ. of Tex., Austin.

Patterson, C. C. and E. F. Gloyna (1965) Dispersi on Measurement in Open Channels. J. of San. Engr. Div., Amer. Soc. of Civ. Engr., 91, SA 3, 17-29.

Pasquill, F. (1962) Some Observed Properties of Medium Scale Diffusion in the Atmosphere. Quart. J. Roy. Met. Soc., 88, 70-79.

Pritchard, D. W. and J. H. Carpenter (1960) Measurements of Turbulent Diffusion in Estuarine and Inshore Waters. Bull. Int. Assoc. Sci. Hydrol. No. 20.

Proudman, J. (1953) Dynamical Oceanography, John Wiley and Sons, Inc., N. Y., 1953.

Richardson, L. F. (1926) Atmospheric Diffusion on a Distance Neighbor Graph. Proc. Roy. Soc., London, 107A, 709.

Richardson, L. F. and H. Stommel (1948) Note on Eddy Diffusion in the Sea. J. Meteor., 5, 5.

Saffman, P. C. (1962) The Effect of Wind Shear on Horizontal Spread From an Instantaneous Ground Source. Quart. J. Roy. Met. Soc., 88, 382-393.

Schonfeld, J. C. (1959) Diffusion by Homogeneous Isotropic Turbulence, Report FA-1959-1, Rijkswaterstaat, The Netherlands.

Shulman, M. D. and R. A. Bryson (1961) The Vertical Variation of Wind Driven Currents in Lake Mendota. Limnology and Oceanography, 6, 3, July, 347-355.

Taylor, Sir G. I. (1921) Diffusion by Continuous Movements. Proc. London Math. Soc., ser 2, 20, 196-212.

Taylor, Sir G. I. (1954) The Dispersion of Matter in Turbulent Flow Through a Pipe. Proc. Roy. Soc. London, 223A, 446-468.

von Weizsacker, C. F. (1948) Das Spektrum der Turblenz bei grossen Reynoldsschen Zahlen. Z. Phys., 124, 614-627.

Wiegel, R. L. (1964) Oceanographic Engineering, Prentice-Hall, Inc., Englewood Cliffs, N. J.